POLITECNICO DI MILANO

Masters of Science in Aeronautical Engineering

School of Industrial and Information Engineering

ROCKET MODE OPERATIONAL ANALYSIS OF A ROCKET BASED COMBINED CYCLE MODEL ENGINE

Supervisor: **Prof. Luciano Galfetti**

Co-Supervisor: **Dr. Giulio Riva**

Master of Sciences Thesis
NOMAN AHMED FRAZ
Matricola: 858868

Milan, April 2018

Academic Year 2017-2018

Contents (PLAN OF PRESENTATION)

LIST OF FIGURES

1 CHAPTER 1 (INTRODUCTION)

1.1 MOTIVATION

The history shows that the aerospace propulsion has passed various phases from the first flight attempt by Wright brothers in 1903 and later on the breakage of sound barrier by Yeager in 1947. This was in fact, a milestone in the history which leaded the attention to the possibility of flight at higher speeds than speed of sound. The desire to fly higher and to fly faster and faster leaded to the first ever flight into the space by Gagarin 1961 being able to defy the gravity, which further abled the man to step on the moon in the same decade later in 1969. The quest for higher and faster travel into the space is not ended and will be continued further at a much higher pace. Especially, the commercial planes have not been gone supersonic after the grounding of Concorde in 2003 following the incidence that resulted in loss of several lives.

However the gas turbines which have been used in most commercial and military airplanes imply several structural and design restrictions because of presence of rotating parts in the engines and hence resulted in achievement of the highest possible speed of Mach 3. For higher speeds in the supersonic region (Mach 3-5) special kind of propelling mechanism is required that is called Ramjet. For even higher speeds(Mach 6-8), supersonic combustions Ramjets are needed. Modern propulsion systems are a result of combination of solid propellent rockets and ramjets to create a Ramjet/Scramjets. These systems are air breathing systems which provide very high specific impulse. The rocket combustor is basically the integral part that serves as a booster and the ramjet engine sustains the operation up to the higher speeds. These systems are highly efficient in terms of propulsive performance, compactness and possess high maneuverability.

There are several types of Rocket-ramjet configurations present today, which include liquid fuel rocket ramjet, solid fuel rocket ramjet and solid propellent ducted rocket systems. There are enormous advantages of ducted rocket including the long flight capability of air-breathing systems. They have the advantage of having high specific impulse, long flight range, easy throttle ability and extreme terminal velocities over the normal rocket engines. Also, the ducted rocket system uses air as the oxidizer for combustion, hence it presents a considerable weight reduction as oxidizer is not required to be carried along. In a typical ducted rocket system, a rocket booster system is required to accelerate to supersonic speed. It presents the need of dual mode combustion chamber. When the velocity is zero, solid propellent is required for the booster rocket, then it becomes the secondary combustor for the sustained operation, with the complete

burning of propellent. A fuel rich gas mixture from the primary combustion chamber is then injected from the secondary combustion chamber with reacts with the incoming air at high temperature which is already being compressed by a system of shock waves at the inlet and is decelerated in the diffuser.

Previous studies performed in such propulsive system on various areas of research along with the experimental investigations to evaluate the parameters like efficiency of combustion, etc. show the dependency on the systems geometry i.e.: inlet angle(air), geometry at the inlet. Several studies have been carried out so far to understand different modes of the said system along with different types of fuels used. Such systems are commonly known as combined cycle(CC) engines as they can modify their operation mode based on the instantaneous velocity of the system and also according to the nature of external environmental conditions. They are also known as Rocket based combined cycle systems which work as pure rockets at low speeds(take off conditions) , ejector rocket from Mach 1.5 till Mach 2 and modify their operation to ramjet as the speed increases from Mach5-6 and finally in scramjet mode in the hypersonic speed range.

This study has the scope towards the analysis of the rocket only mode operation of a Rocket based combined cycle engine in the supersonic and possibly in the hypersonic speed ranges in a research facility near Milano, Italy called Consiglio Nazionale delle Ricerche (CNR) on a model engine with the simulation of the same operating conditions as of the space environment in the laboratory.

1.2 OBJECTIVE

The objective of this thesis is to study the Rocket based Combined cycle engine in detail with the development of sound knowledge of the Rocket mode operation of RBCC model engine. Several tests were performed on the ramjets and scramjet mode in the high enthalpy pulsed tunnel of CONSIGLIO NAZIONALE DELLE RICERCHE (CNR) based in Milano using a parametric model engine, with modifiable configurations depending upon flow properties of the fluid in the facility. Preliminary tests up to Mach 8 were carried out for the simulated flight conditions in the facility and detailed characterizations of the engine. A detailed study using the same parametric engine is presented by Riva Giulio et al. [1] at Mach 4.5.

The aim of this study is to focus on the data acquired from the tests with PURE ROCKET MODE operation, for different values of fuel and oxidizer mass flow rates and hence equivalence ratio, for two different configurations of Ramjet and Scramjet combustion chamber. The result from the test was recorded using a state of the art data acquisition system and was analyzed using the FORTRAN codes for the calculation of Thrust, Mach numbers at various location and the specific impulse, using different evaluation techniques which are discussed in detail in the following sections of the thesis.

2 CHAPTER 2

2.1 STATE OF THE ART

2.1.1 RAMJET ENGINE SETUP

Ramjet is an air breathing engine that operates between Mach 2 and Mach 5 having a maximum efficiency around Mach 3. Extensively used as missiles propeller and shells, they propose several benefits upon normal rockets as they do not carry oxidizer, which results in significant weight reduction, they offer simplicity of design with much higher efficiencies over a large flight range with high maneuverability and efficient cruise and acceleration properties with the ability to modulate thrust.

2.1.1.1 DESCRIPTION

A simplest jet engine, without any rotating parts such as turbomachines and uses its geometrical characteristics to compress and to accelerate intake air by an effect called as RAM effect. It cannot be operated from the rest, hence there is a need of another mean of propulsion such as rocket.

Ramjet engine can be divided into the different parts such as inlet, diffuser, combustion chamber and the outlet nozzle. Inlet is designed in a way to act as the compressor , thanks to the shape as a diffuser. As the vehicle moves faster, more compression is achieved. The compressed air is then fed into the combustion chamber where mixing with the fuel takes place.

A spark plug ignites the mixture which produces the thrust. A flame holder is present in order to stabilize the flame for a stable ignition to provide a continuous thrust. Combustion increases the enthalpy of the gas, which then expands through the nozzle resulting on the net thrust.

The **thermodynamic cycle** of the Ramjet is:

- Compression(adiabatic) : ramjets exploit very high dynamic pressure recovery from the air approaching the inlet diffuser. Intake recovers efficiently, the stagnation pressure to a very high value resulting in compression of the air.
- Heat addition(Isobaric): compressed air is mixed with the fuel.
- Expansion(adiabatic): The nozzle recovers the kinetic energy from the high temperature combustion products to produce net thrust.

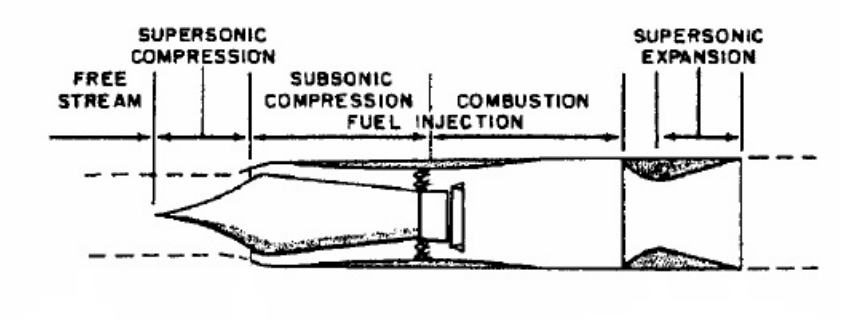

Figure 2:1: Schematics of a generic RAMJET engine

2.1.1.2 DESIGN

There are several factors which needs to be taken in account while designing of the ramjet engines such as internal pressure in the duct, the body temperature and dynamic pressure load.

The requirements for the adequate amount of static pressure in the combustion chamber to get maximum combustion efficiency and to get sufficient are critical. With the increase in speed, compression requirements are less. The design requirements include the problems of low combustion efficiency and limited equivalence ratio ranges and material selection considering the high pressures and temperature limits. In the high Mach region, extreme dissociation takes place, where the compression could be influenced by the non-equilibrium flow which results in the distortions in the inlet flow. Its effect is a region with less compression efficiency at very low Mach number.

2.1.1.3 RAMJET COMBUSTION CHAMBER

Combustion chamber of a ramjet has several important elements to guarantee the complete and stable chemical reaction. Primary combustion chamber produces a flame that provides the ignition of fuel/air mixture. A spark plug ignited the mixture in the primary combustion chamber, where fuel is injected separately from the main feeding line to ensure a higher combustion efficiency and stable operation. Primary chamber may or may not be present depending upon the operation, but there is always a need of flame holders to ensure stable reaction. These are non-aerodynamic bodies to create stronger local ignition, and are always active. Design of combustion chamber is done in a way to

recirculate the combustion products after the stabilizers which enhances the mixing of air and fuel.

Two main regions of flow are characterized in the combustion chamber of a ramjet engine:

- Annular duct formed by the flame tube and the outer duct, representing the cooling flux.
- Flame tube section, which take direct part in the combustion.

With Higher speeds of main flux (of order 100m/s), as compared to a turbojet combustion chamber but with a very less pressure loss coefficient which is a hurdle to the combustion of fuel in the chamber. This leads to a longer length of ramjet combustion chamber as compared to that of a typical turbojet engine. A tradeoff is required when designing the combustion chamber.

2.1.1.4 IGNITION AND EXTINCTION PROPERTIES

Figure 2:2 shows the ignition and extinction properties of the combustion chamber of a typical ramjet engine. Engine can operate in the ignition portion. Ignition is not possible in the single line portion but the engine can operate. Pressure P_2 implements a significant effect on the ignition process as when it decreases, it restricts the ignition region to a very small portion and may lead to its disappearance

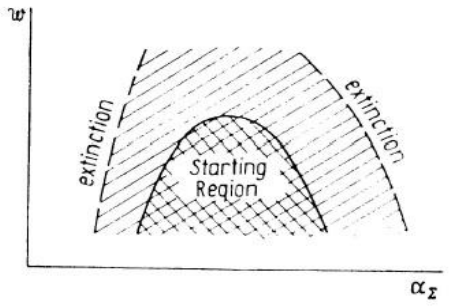

Figure 2:2:Ramjet Ignition and Extinction Properties

2.1.1.5 CLASSIFICATION:

Classification can be done according to fuel type (either solid or liquid) and the type of booster application.

- Liquid fueled ramjet (LFRJ) uses a hydrocarbon fuel, injected before the flame holder in the combustion chamber, to stabilize the flame after ignition. The fuel is typically pressurized, which makes the system complicated and is more expensive.
- Ramjet requires a booster from rest to the speed from where its intake can start working efficiently. Which are normally solid propellent rockets, either in tandem or wraparound. Tandem booster is mount at the aft body of ramjet which increases the length of the engine, whereas the later has multiple boosters wrapped outside the engine hence increasing the diameter of the system resulting in higher drag.
- The integrated booster applications have the propellent, casted in the combustor, hence providing an efficient packaging solution. Same approach can be used on both solid & liquid rockets. Integrated rockets are complicated due to various requirements for the nozzle for boost and ramjet phases. A separate nozzle is utilized, and ejected after booster burnout. However, Some designs require nozzle less operation.
- Another method to get thrust at zero speed is to exploit the supersonic exhaust from a rocket combustion chamber at the inlet of the ramjet engine.
- Solid fueled integrated rocket ramjet (SFIRR) utilize the solid fuel casted on the outer wall of ram combustor. Fuel is injection from the ablation of propellant by the hot compressed air at the intake. They are preferred over LFRJ due to simplicity, but provide a problem when throttling is required
- A fuel rich gas is burnt in the main combustion chamber of ramjet with the compressed air from the atmosphere. Gas flow enhancing the mixing efficiency and hence the pressure recovery.
- A throttleable ducted rocket, sometime called as variable flow ducted rocket, utilizes a valve which permits the gas generator exhaust to be throttled enabling the thrust control. Such a system is much simpler than LFRJ.

2.1.2 SCRAMJET (SUPERSONIC COMBUSTION RAMJET)

A hypersonic propulsive system in which a supersonic flux achieved by the energy gained by the combustion of fuel-air mixture.

2.1.2.1 Description

A typical ramjet has a system of shock waves at the inlet to slow down the air flux to subsonic range. Whereas scramjets do not require the air flux to be subsonic, hence the requirement of the throat section is no more present. We can achieve hypersonic speeds

of Mach >6. Theoretically speaking, there is no higher limit for the speed, but in practical terms, it is difficult to go beyond Mach 10-11 as at such speeds, the engine becomes sensitive to the small anomalies and stable supersonic combustion operation becomes extremely difficult.

2.1.2.2 DUAL MODE

Many systems use the dual operation of scramjet-ramjet. Such system have the ability to work as Ramjet for lower Mach numbers () and as scramjet for higher Mach numbers.

RAMJET mode: It has subsonic flux at the inlet, transition to supersonic though a constant diameter diffuser known as isolator. Then there is a throat section, which enables to keep the flow subsonic. This leads to normal shock train. Dual mode requires the a second throat area due to thermal choking, by several factors such as area and fuel-air mixture.

SCRAMJET mode: It excludes the requirement of a throat area. The system modifies its shape by removal of the throat area. The isolator which separates the inlet from the combustion chamber. To avoid the production of the pressure gradient in the combustion chamber of the scramjet which could leads to the separation of boundary layer in the presence of high pressure gradient makes the engine not able to start, isolator plays an important role, as it compensates the creation of an opposite pressure gradient when the area increment (of the Engine) is not sufficient to provide the thermal choking. Isolator prevents high opposite gradient and guarantees the smooth start of the scramjet engine.

2.2 HISTORICAL EVOLUTION OF RAMJET & SCRAMJET

Several studies have been carried out beginning from early 19th century with significant contribution in development of the concept of supersonic and hypersonic speed vehicles.

2.2.1 RAMJET

- The concept was presented in earl 19th century, with first tests conducted after 30 years. Many researchers focused on the problem of reducing the thrust to eight ratio of the engines. French (Lorin) and U.S.(Lake) along with their co-researchers worked on the ramjet ejectors for the first time in the history. Lake was pioneer to present the very first patent in 1909. Lorin's publication regarding ramjet date back to 1913.
- First practical ramjet model with the shock waves at the inlet due to its characterized shape was patented by Carter from the Britain in 1926. 2 years Later, first LFRJ with a conical nose was patented by Hungarian scientist Fono. Germans started to use the concept in military application in 1930s which were able to achieve Mach 2.9-4.2. Germans were able to make the first operational ramjet powered missile called V-1 buzz bomb, which was launched by an aircraft.
- Russians also tested ramjet up to Mach 2. In 1939, they were able to obtain a successful test of a tandem boosted ADR solid fueled rocket.
- World war II leaded to several development efforts to produce aerially guided missiles in US and Great Britain which continued to the evolution of several weapon systems like BOMARC, Talos(US) & Bloodhound(G.B.) missiles.
- Many engines were designed by Russian in 1960s including SA-4 and SS-N-19 based on ramjet configuration.
- Worldwide development of many missiles systems was carried out in 1980s which included Missile Probaoire Stato Rustique(MPSR), VESTA, Supersonic low latitude target(SLAT), low range ant ship Hsiung Feng, antiradiation missile ARMINGER and many other systems.

2.2.2 SCRAMJET

- Hypersonic field research was carried out mostly in the 20th century. First generation scramjets were developed and tested in U.S. in mid 1960s. utilizing hydrogen based fuel, several tests were performed by U.S Navy. Later on, the hydrocarbon based fuels were also tested.

- Second generation scramjets were developed and tested in US in 1970s with the achievement of Mach 7,with the detailed evaluation of its performance. Wind tunnels tests up to Mach 8 were conducted.
- Third generation scramjets were introduced in 1986 by the studies performed in Germany and Russia.
- Later on, under the NASP program of U.S. hydrocarbon fuels were examined and NASA started the use of Air Breathing combined cycle Engine.
- Queensland university started the study of Scramjet in 2002 with the project name HyShot.
- American HyperX team developed the very first functional Scramjet maneuverable thrust product engine(X-43A) which leaded to the new era of evolution of the supersonic combustion engines. Several studies are being performed in the various parts of the world to understand the characteristics of the SCRAMJETS.

3 CHAPTER 3

3.1 TEST RIG SETUP-ROCKET BASED COMBINED CYCLE (RBCC) ENGINE

RBCC engines are air breathing systems with the ability modify their mode of operation depending upon the instantaneous speed of the vehicle and external environment. With pure rocket operation at Mach 1.5-2, changes to Ramjet from Mach 5.0-6.0, scramjet in the hypersonic velocity range and again as pure rocket outside the environment.

The concept of the setup was already studied by [2] in a larger facility and provides an effective solution to perform conversions between different operation modes. Engine has the ability of making transitions between Mach number of 4 to 7 by changing its geometry depending upon the requirement. The system exploited the rectangular geometry, making it possible to easily adapt by simple sidewall transitions with the change of speed of flight. The system has a low speed combustion chamber, followed by a con-di nozzle as a typical ramjet setup. Design of the inlet has the ability to inject fuel from a separate source required to allow the system to work as a pure rocket or as the igniter system for the Ramjet mode. Inlet section has a width of 10cm whereas the exhaust being 14cm wide, with a constant height of 4cm, and the length of the system goes up to 1.06m.

When it came to material selection, the walls were made from stainless steel, whereas Aluminum was exploited for the model support structure. The system is able to work as Pure-Rocket injector, Ramjet or scramjet modes by making changes in the internal geometry by slight modifications carried out by the translations of the side walls. Compression section of the engine was designed by making a tradeoff in order to make the system able to operate as a scramjet at higher Mach numbers.

The preliminary test results have confirmed that the system can be modified easily to cover the scramjet as well as ramjet operation modes. To carry out such changes, the model has two parallel plates on the top and bottom, whereas the sidewalls can translate without any constraints in between the top and bottom plates, the compressor internal walls are provided by the central strut.

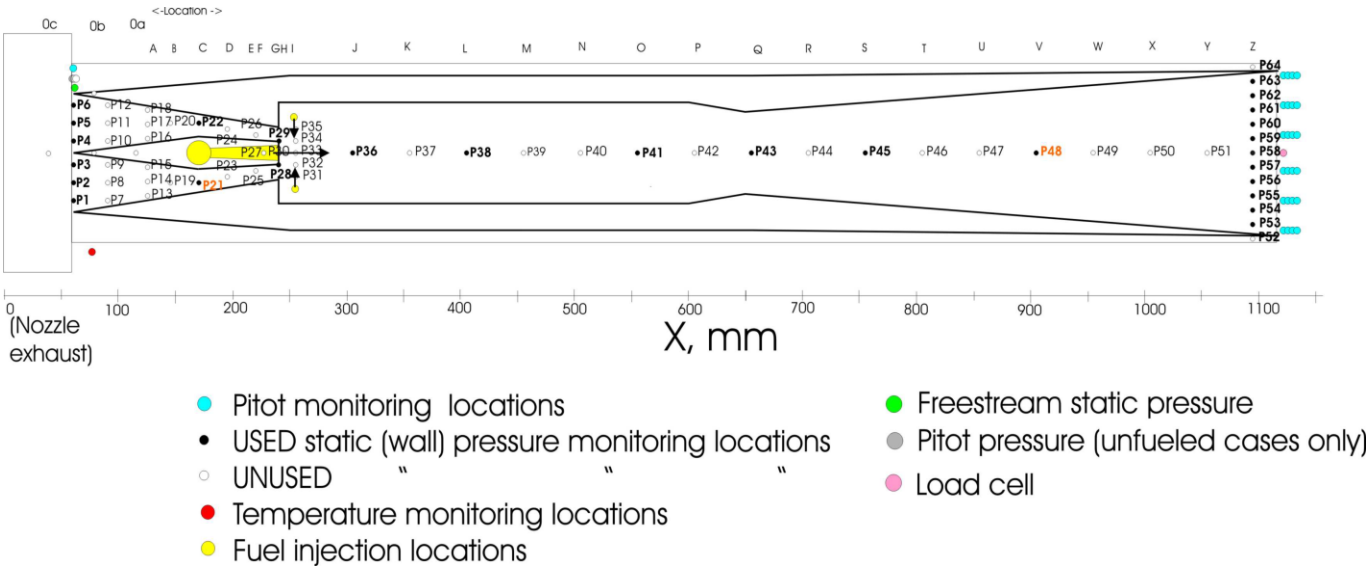

Figure 3:1 Top View of RBCC model Engine showing locations of the pressure and temperature sensors

A rocket motor is present in the central strut represented by F1 in Figure 3:1 which is fueled by hydrogen and oxygen gases through calibrated sonic hole. Rocket has a cylindrical combustion chamber with a total volume of 10cm^3. The purpose of the rocket is to inject the combustion products or pure hydrogen in the ramjet combustion chamber. Three divergent equally spaced nozzles are present at the inlet of the ramjet combustion chamber. The top plate incorporates the spark plug to ignite the rocket fuel and the connectors to fuel injection in to the main ramjet combustion chamber(secondary) which is normally operated by another solenoid valve and is totally separated from the operation of the rocket.

The secondary injection ports are located downstream of the primary combustion chamber inlet, aligned symmetrically with respect to the vertical midplane of the engine. Fuel is fed perpendicularly to the direction of the flow through two 4cm long and 0.6cm in diameter pipes attached to the top walls through 6 equally spaced holes as shown in the Figure 3:2.

.

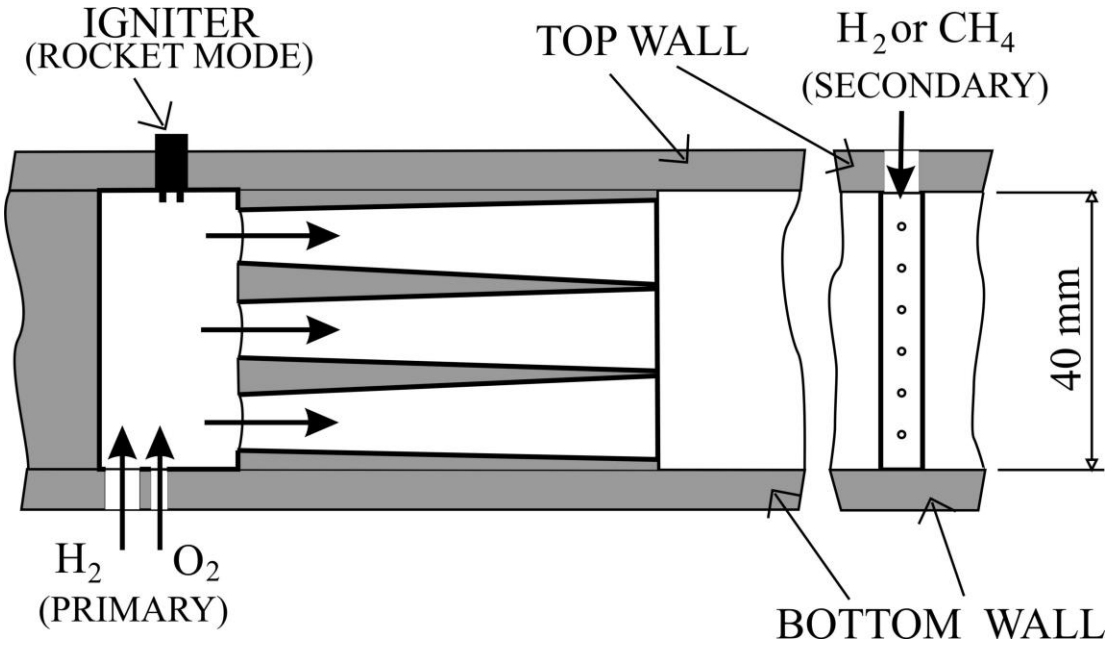

Figure 3:2 Schematic of Primary & secondary combustion chamber of the engine

A load cell is used to maintain the engine in its original position which allows the axial movement only with the help of rails system and measures the axial component of the thrust increment output. Several tests were performed both fueled and unfueled under the same conditions for the operation.

Leading edge of the bottom plate extends 6cm upstream, as to measure the static pressure at the inlet. The compressor section divides the 10cm wide into two equal sections. Central strut 18cm long with an upstream section of 11cm in length, has a 15° total wedge angle is followed by converging section of 7cm in length. Strut back face is 2cm wide, with each side wall with an angle of 7.5° over the total 18cm length of the section. The main compression is done in the first 11cm, where the later portion offers a modest reduction. Geometry contraction ratio is equivalent to 0.32, which is comparatively lower than that of the operations performed by Kantrowitz et al. [3] .

In order to have the supersonic operation of the compressor, a pulsed start is employed using the flow release from the facility nozzle. Combustion isolation requires considerable increase of the area at the inlet of the combustion chamber with 75° expansion ramps. Combustion chamber has a constant area of $35cm^2$ with a width of 12cm and is followed by a convergent nozzle having a throat(9cm) at 41.5cm downstream of the strut and a divergent portion extending up to 46.5cm and an exhaust that is 14cm wide.

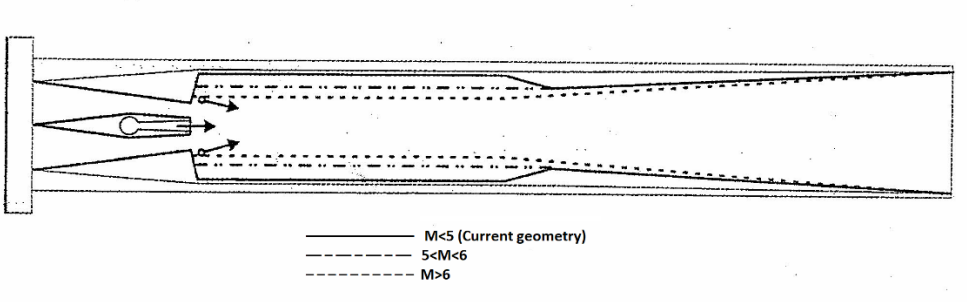

Figure 3:3 Expected changes of geometry of the Engine for different Mach number

Figure 3:3 shows a sketch of the geometrical expectation of the geometry with the change of the flight conditions. Sufficient temperature recovery is possible for higher flow speeds in the combustion chamber by increasing the Mach number with the removal of convergent part of the exhaust nozzle. Recent research work going on in the CNR-IENI involves the study of the behavior of the system without the throat.

An older version of the facility [4] used a 100 liters volume compressor(free piston type) with a 50 liters volume reservoir with a long pump tube to provide the compressed air into a stagnation vessel, which provided the necessary enthalpy to simulate the Mach 4-5 flight conditions. The stagnation vessel followed a conical nozzle, whose geometry can be modified to simulate the required Mach number. The test chamber is followed by a large dump tank of about 22000 dm^3 , maintained at low pressure around 1mbar. When there is a need to modify the nozzle operation, the dump tank can be moved by the help of an electrical motor and a rail. Clean air test flows at low Mach numbers were obtained using compressor only.

After examining the results, the conclusion drawn was that the compressor is unable to feed enough air mass in to the stagnation vessel, also the enthalpy level to simulate the condition was not enough. This resulted in adoption of the hydrogen pre-combustion as a solution to the above problem, which increased the test gas enthalpy to the required level. Hence the original stagnation vessel was replaced by a constant volume combustion chamber with the inlet fuel ports and several spark plugs to start combustion. Hydrogen combustion produced the vitiated air . Air, oxygen and hydrogen filled in the facility nozzle was combusted by a multiple spark plug system that enabled the repeatability and minimized the combustion time. The combustion products(21% Oxygen & 11.5% H_2O vapor) when introduced into the test chamber through a pressure driven valve, produced the required nominal flight Mach number of the flow to simulate the required environment for the tests.

3.2 DATA ACQUISITION SYSTEM

The test facility is equipped with wall mounted static pressure sensors on the bottom plate at several location. Static and pitot probes at the inlet section provide the actual freestream properties of the flow(static and stagnation pressure) which confirms the uniformity of the flow produced by the facility nozzle. Stagnation gas temperature is taken from a probe of iridium(80microns diameter) based on the electrical resistance change. The data from the probe was corrected for possible heat loss due to radiation and conduction to the supports and the locations of electrical connections. To detect the inlet flow temperature, Pt/Pt-Rh thermocouples(50 microns diameter) were rarely used which needed to be replaced after a few tests. Evaluation of total enthalpy of the gas and momentum was carried out though the combination of the pressure measurements from various locations and by the computation of Mach number distribution.

Temperature probes were also mounted on the exhaust but only during unfueled tests, results were acceptable as unburnt fuel reacted with the probe and altered the measurement in fueled tests.

Average Mach number could also be obtained by using mass conservation equation and compared with the one obtained from pressure probes data which resulted in $\pm$2% difference in both the values. A 5000 N load cell measured the axial force which enabled to get the thrust increment for fueled tests. Piezo resistive transducers (natural frequency 100 kHz or higher) were used to measure pressures. Data Acquisition system utilized 12bit with 64 channels with a sampling frequency of 20kHz and the acquisition time set at 1s.

NOTE:

The results from one of the sensors at the location “V” were suspicious and on investigation, it was found out that the sensor has burnt out due to some unknown reasons, hence its reading were totally discarded in all the tests performed at the facility. The sensor replacement required a long procedure and would have led to the delay with respect to devised schedule for the tests in the facility.

3.3 PURE ROCKET OPERATION OF RBCC ENGINE

In order to study the Rocket mode only, initially a vacuum environment is created inside the flow channel. The Rocket combustion chamber was fed with the fuel and oxidizer which were kept at some specific pressures (10,12,15 & 20 bars for different tests) and at room temperature. Two different configurations were tested using the same operating conditions with & without firing of the spark plug (referring to study of the setup with & without combustion). This is to be noted here that during pure rocket mode, the ramjet combustion chamber is not operational and hence no fuel is fed in to ramjet combustion chamber and the system works as a simple rocket. Pressure measurements were observed to be stabilized within a span of few milliseconds indicating the quasi-steady behavior of the flow. The injection pressures of fuel and oxidizer (Pressure of hydrogen reservoir =10 bar, pressure of oxygen reservoir= 16 bar, test with combustion-TEST case : H10-O16-s1) plotted against time, also the rocket combustion chamber pressure measurements during one of the tests are shown in the

Figure 3:4.

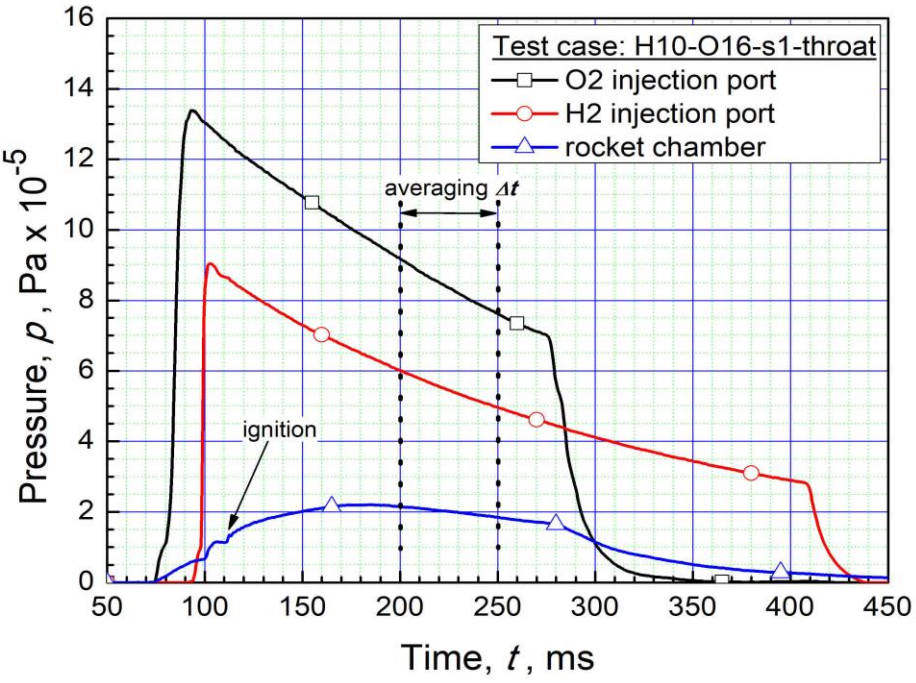

Figure 3:4 Fuel and oxidizer injection pressure along with the ignition characteristics after the firing of the spark plug vs time history

Figure 3:4, clearly shows that H2 & O2 were fed into the primary chamber to operate the system in pure rocket mode for about 400ms. The fuel supply refers to the a blow out process and the pressure of the reactants can be observed to be decreasing during the test. At around 300ms, the supply of oxygen is cut-off and only fuel is fed in order to cut off the rocket mode. Equivalence ratios were kept nearly constant during the complete test . Measured injection pressure values enable to evaluate the time history of fuel injected mass flowrates assuming the isentropic discharge and sonic ports. The discharge coefficient was defined by static measurements before and after the fuel injection, under thermal equilibrium and is compared to mass flow rates obtained from the pressure data of the injection ports.

3.4 TEST PROCEDURE

A series of tests were performed in the facility in which primary injection system was operated as a pure rocket for different air to fuel ratio and hence equivalence ratios, for two different configurations of ramjet and scramjet combustion chamber.

Vacuum tests were carried out without the flow of any gas through facility nozzle, while fuel and oxidizer being hydrogen(stored in 2300cm^3 reservoir) and oxygen(252cm^3 reservoir) at room temperature. Multiple port injection system enhanced the mixing. Overall area of the oxygen and hydrogen injection ports 6.28mm^2(discharge coefficient 0.763) and 12.57mm^2 (discharge coefficient 0.808) respectively. Rocket is fed simultaneously fed by fuel and oxidizer supply, whose ratio is kept nearly constant in time. The acquired data set include the fuel and oxidizer injection pressure, primary injector pressure, wall pressure at different locations and exhaust pressure at different locations of the nozzle.

The required mass flow rates are obtained by regulating the fuel and oxidizer reservoir pressures and vacuum is obtained in the test chamber with pressure less than 50 Pa. Solenoid valve is used to feed oxygen into the chamber with opening time 200ms , which is followed by hydrogen feed after approximately 20ms (opening time 300 ms) as shown in Figure3:4. Combustion tests require a spark plug to ignite the mixture. Both fuel & oxidizer port are kept sonic.

Combustion lasts until the oxygen cut off, but to stabilize the combustion, a long transient time is required because of heat transfer to the walls until the walls attain a less penalizing temperature. Averaging time interval is kept at 50ms and the start of engine leads to a transient and then finally a quasi-steady operation is attained.

Wall mounted pressure sensors recorded a set of data throughout the test procedure and the measured values plotted against time are shown in Figure 3:5. The locations of the sensors are marked in Figure 3:1 in detail.

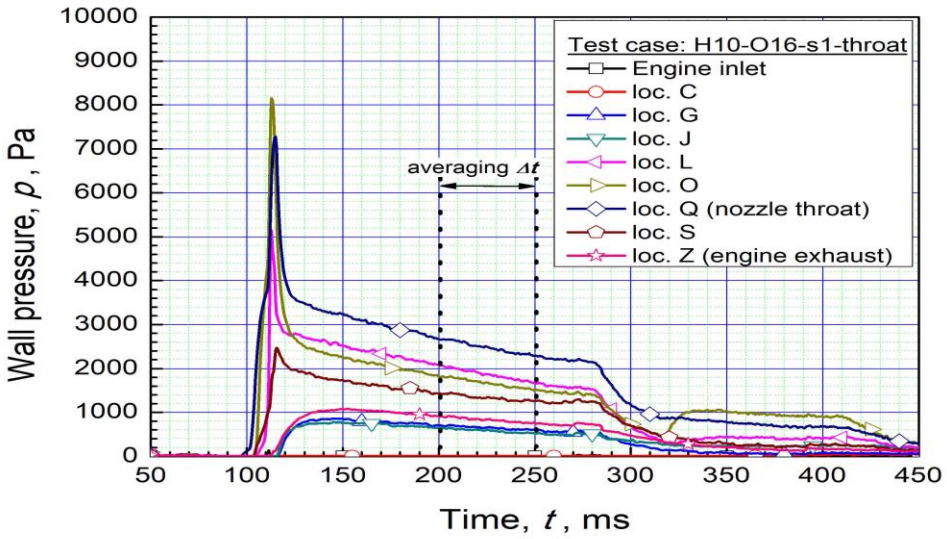

Figure 3:5 Time history of pressure sensor measurements in pure rocket operation mode

It is evident from the above figure that gas from the rocket-injector nozzle do not flow back in to the compressor section as zero pressure is maintained at the “C” location as well as at the inlet section. Downstream location experience a sudden rise in the pressure followed by a consistent drop in time during the reactants reservoirs blow-down. Highest value of quasi-steady pressure was found at “Q” which is the throat of the ramjet configuration, which leads to the fact that supersonic flow is achieved at the ramjet combustion chamber and the nozzle.

A strut with 24 pitot probes is mounted at the exhaust section to cover entire area of exhaust. The data set, along with the wall pressure data is used to evaluate the Detailed

Mach number distribution and the momentum of the flow, leading to the Engine thrust. A load cell gives a direct measurement of Engine thrust which is shown Figure 3:6 along with the fuel and oxidizer mass flow rates time histories.

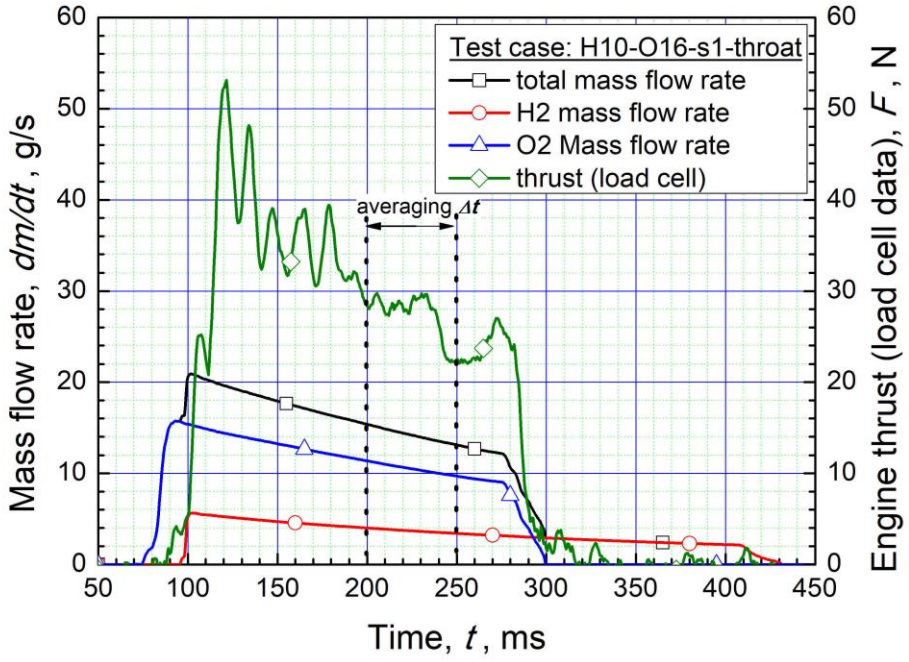

Figure 3:6 Load cell output(thrust) & mass flow rates of reactants throughout the operation

3.5 DATA ANALYSIS

ASSUMPTIONS

The following assumptions are being made in order to carry out the analysis of the rocket only mode of the facility.

- It is being assumed that the time histories of the reactants injection and combustion chamber stagnation are known.
- Rocket thrust is also available to compare the results.
- Equivalence ratio & the mass flow rates of the reactants are regulated by the initial pressures of their reservoirs.
- Both the injection ports are sonic and the reactant discharge is adiabatic.
- Both the reactants act as ideal gas.

Time histories of Thrust, combustion efficiency ,Specific impulse, , Equivalence ratio and Specific thrust can be evaluated using the output data set. With 1ms time step, engine performance analysis is carried out in detail.

All the correlations used in this analysis are derived from standard thermodynamic relations or conservation equations [5]. In order to get the stagnation temperatures of the two volumes, following relations can be used starting from the room temperature(300K).

$$T_{t,f} = 300\left(\frac{p_{t,f}}{p_{t,f,max}}\right)^{\frac{\gamma_f - 1}{\gamma_f}} \qquad 3\text{-}1$$

$$T_{t,ox} = 300\left(\frac{p_{t,ox}}{p_{t,ox,max}}\right)^{\frac{\gamma_{ox} - 1}{\gamma_{ox}}} \qquad 3\text{-}2$$

Using the stagnation properties of the flow. Mass flow rates can be computed. Choked flow is established

as the pressure at the intake ports is larger than the critical value, hence relations for the mass flow rates

are as follow:

$$\dot{m}_f = A_f \frac{p_{t,f}}{\sqrt{T}_{t,f}} \sqrt{\frac{\gamma_f}{r_f}} \left(\frac{2}{\gamma_f + 1}\right)^{\frac{\gamma_f + 1}{2(\gamma_f - 1)}} \qquad 3\text{-}3$$

$$\dot{m}_{ox} = A_{ox} \frac{p_{ox,f}}{\sqrt{T}_{ox,f}} \sqrt{\frac{\gamma_{ox}}{r_{ox}}} \left(\frac{2}{\gamma_{ox}+1} \right)^{\frac{\gamma_{ox}+1}{2(\gamma_{ox}-1)}} \qquad 3\text{-}4$$

The above formulation is based on the assumption of the sonic flow achieved at the injection ports.

However, there could be some cases where the critical pressure is higher than the pressure across both ports. For the sonic case, pressure measurement from the upstream stagnation pressure is taken. For the latter case, pressure on the port is assumed to be downstream pressure, and the isentropic expansion gives the flow Mach number in the port. Mass flow across non chocked section is given by:

$$\dot{m}_{port} = \rho * v * A *= \frac{p * M * A *}{\sqrt{T *}} \sqrt{\frac{\gamma}{R}} \qquad 3\text{-}5$$

$$p *= p_{down} \quad (assumed) \qquad 3\text{-}6$$

Subscripts up and down represent the port upstream and downstream stagnation condition respectively. Mach number and the stagnation temperature at the throat section is given as

$$M_* = \sqrt{\frac{2}{\gamma - 1} \left[\left(\frac{p_{up}}{p_*} \right)^{\frac{\gamma-1}{\gamma}} - 1 \right]^1} \qquad 3\text{-}7$$

$$T_* = \frac{T_{up}}{1 + \frac{\gamma - 1}{2} M_*} \qquad 3\text{-}8$$

Mass conservation equation after substitution, can be applied to non-choked reactants ports with the assumption of reactants stagnation conditions as upstream and rocket combustion chamber conditions as downstream, which can be given as

$$\dot{m}_{port} = A_* \frac{p_{down}}{RT_{up}} \sqrt{\left(\frac{p_{up}}{p_{down}} \right)^{\frac{\gamma-1}{\gamma}} \left(\left(\frac{p_{up}}{p_{down}} \right)^{\frac{\gamma-1}{\gamma}} - 1 \right) \frac{2\gamma RT_{up}}{\gamma - 1}} \qquad 3\text{-}9$$

The total mass flow rate is given as

$$\dot{m}_{tot} = \dot{m}_f + \dot{m}_{ox} \qquad 3\text{-}10$$

With the known exhaust gas composition, choked flow conditions across the rocket exit are assumed to get the combustion chamber temperature. The combustion in the chamber cannot be considered as complete combustion considering the gas residence time in the chamber very short, also partial mixing of the reactants. A new parameter is necessarily introduced known as combustion efficiency depending on the quality of combustion in the combustion chamber.

Chemical reaction occurring in the combustion chamber considering only Hydrogen and oxygen can be written as:

$$a\ O_2 + b\ H_2 \rightarrow c\ O_2 + d\ H_2 + e\ H_2O \qquad 3\text{-}11$$

In the above equation, a & b represent the moles of oxygen and hydrogen are known from the air fuel ratio whereas c, d & e are unknowns and their values depend on the reaction completeness (i.e. η_c: combustion efficiency). η_c is assumed to be a known parameter which is determined later by iterative technique. In order to get the correct results, calculations for lean and rich mixtures are performed separately.

3.5.1.1 RICH MIXTURES

Considering complete reaction(η_c =1) relates to zero oxygen left in the chamber (c=0) while no reaction leads to c=a. Rich mixture is represented by using subscript “r”.

Hence the values for c, d and e can be written as :

$$c_r = a(1 - \eta_c) \qquad 3\text{-}12$$

$$e_r = 2a\eta_c \qquad 3\text{-}13$$

$$d_r = b - 2a\eta_c \qquad 3\text{-}14$$

3.5.1.2 LEAN MIXTURES

With no hydrogen left in the products leads to y=0; whereas no reaction y=b, we obtain as follow:

$$d_l = b(1 - \eta_c) \qquad 3\text{-}15$$

$$e_l = b\eta_c \qquad 3\text{-}16$$

$$c_r = a - \frac{b}{2}\eta_c \qquad 3\text{-}17$$

The result from the above analysis requires the assumption of steady or quasi-steady gas flows through the rocket, which characterizes that the coefficients used in the calculations (a, b, c, d & e) are the volume flow rates (mole/s) of the reactants and the products.

The table 1 summarizes the above discussed chemical reaction for both conditions.

REACTANTS : O_2-H_2	$\boldsymbol{a\,O_2 + b\,H_2 \rightarrow c\,O_2 + d\,H_2 + e\,H_2O}$		
	c	**d**	**e**
RICH MIXTURE	$a(1 - \eta_c)$	$b - 2a\eta_c$	$2a\eta_c$
LEAN MIXTURE	$a - \frac{b}{2}\eta_c$	$(1 - \eta_c)$	$b\eta_c$

With the known chemical composition of the products and reactants, and the combustion chamber pressure p_t, mass conservation equation can be used to get the stagnation temperature in the combustion chamber (assuming choked flow in the nozzle).

$$T_{stagnatioon} = \frac{\gamma}{r}\left(\frac{p_t A_{th}}{\dot{m}}\right)^2 \left(\frac{2}{\gamma + 1}\right)^{\gamma+1/\gamma-1} \qquad 3\text{-}18$$

In order to get the actual value of combustion efficiency, we compare the actual energy release rate with the maximum possible energy released by complete consumption of any of the reactants. Rate of energy release is given as :

$$\dot{Q}_c = \dot{m}\, C_p\left(T_t - T_{t,i}\right) \qquad 3\text{-}19$$

While stagnation temperature at the inlet is

$$T_{t,i} = \frac{\dot{m}_f T_{t,f} + \dot{m}_{ox} T_{t,ox}}{\dot{m}} \qquad 3\text{-}20$$

Whereas the maximum energy released is given by the following formulations:

$$\dot{Q}_{c,max} = \dot{m}_f Q_f \qquad \textit{For ER}\leq\textit{1, lean mixtures} \quad \textit{3-21}$$

$$\dot{Q}_{c,max} = {\dot{m}_f Q_f}/{ER} \qquad \textit{For ER}\geq\textit{1, rich mixtures} \quad \textit{3-22}$$

The equivalence ratio is given as

$$ER = \frac{m_f}{m_{ox}}\left(\frac{m_{ox}}{m_f}\right)_{st} \qquad 3\text{-}23$$

Now based on the above description, the combustion efficiency can be defined as:

$$\eta_c = \frac{\dot{Q}_c}{\dot{Q}_{c,max}} \qquad 3\text{-}24$$

The convergence to a final value of combustion efficiency requires several iterations. The following Figure 3:7 summarizes the iterative procedure to get the combustion efficiency.

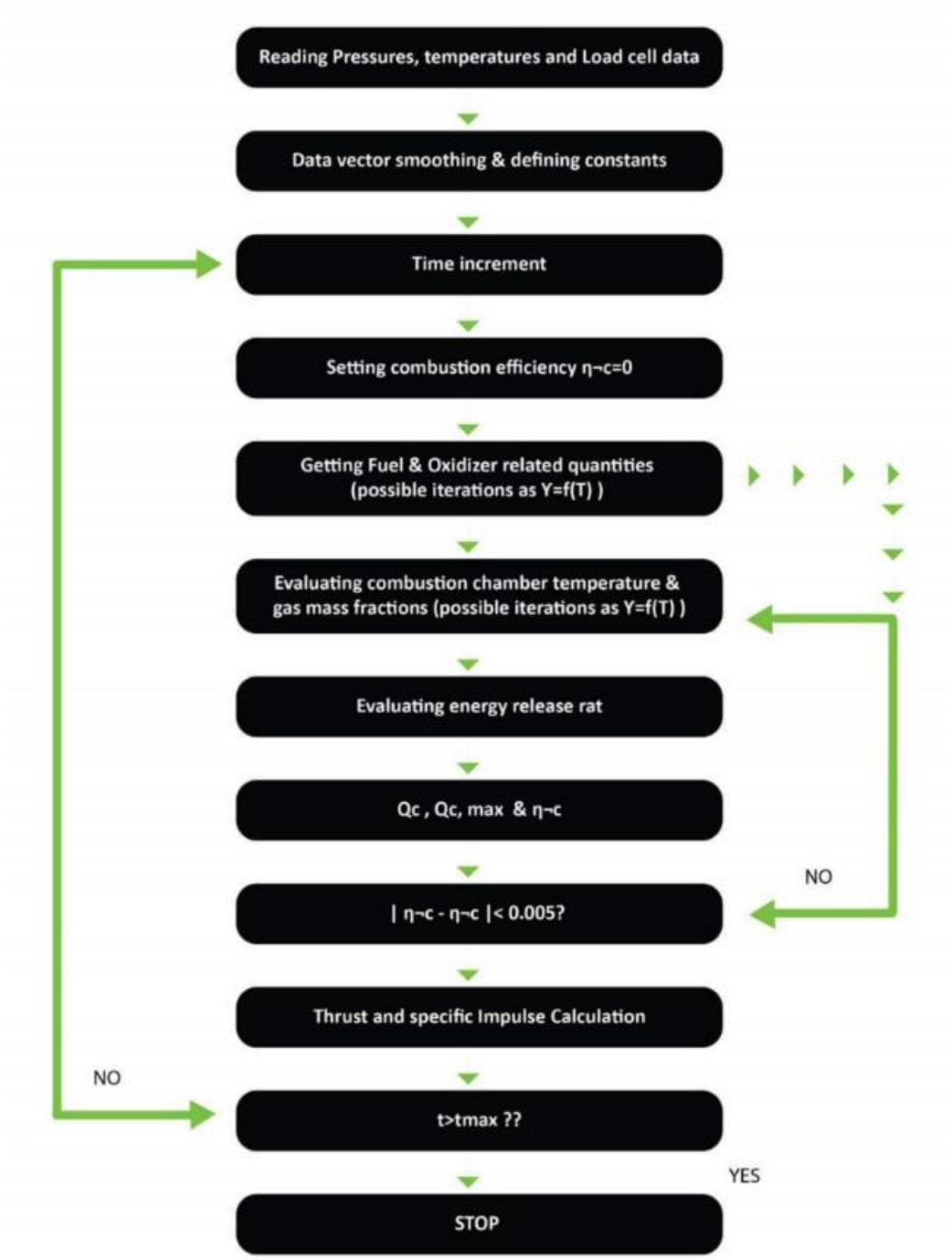

Figure 3:7 Flow chart showing iterative procedure for evaluation of combustion efficiency

Using the mentioned iterative procedure, Rocket thrust and Specific impulse can be evaluated easily. Exhaust Mach number can be computed numerically as:

$$\frac{A_e}{A_{th}} = \frac{1}{M_e}\left(\frac{1+\frac{\gamma-1}{2}{M_e}^2}{\frac{\gamma+1}{2}}\right)^{\frac{\gamma+1}{2(\gamma-1)}} \qquad 3\text{-}25$$

Assuming p_j as the external nozzle pressure, thrust can be given as

$$F_{rocket} = p_r A_e\left(1+\gamma {M_e}^2\right)\left(1+{M_e}^2\frac{\gamma-1}{2}\right)^{\gamma/\gamma-1} \qquad 3\text{-}26$$

Engine exhaust pressure can be replaced by combustion chamber pressure using the isentropic correlations.

$$\left[\frac{\gamma(\gamma-1)p^2A^2}{2R}\right]M^4 + \left(\frac{\gamma p^2A^2}{R}\right) - \dot{m}^2T_t = 0 \qquad 3\text{-}27$$

Wall pressure probes and the pitot probes at the exhaust allow a detailed analysis of the flow. Engine centerline pressure data cannot be considered as a good representation of the average value, but it gives a rough idea about the local nature of the flow. Local Mach number can be evaluated using the following bi-quadratic equation with the knowledge of instantaneous mass flow rate & cross sectional area.

$$\frac{p_{pitot}}{p_{static}} = \frac{\left[\frac{(\gamma+1)}{2}{M_i}^2\right]^{\gamma/\gamma-1}}{\left[\frac{2\gamma{M_i}^2-(\gamma-1)}{\gamma+1}\right]^{1/\gamma-1}} \qquad 3\text{-}28$$

The above equation is valid under the assumption of perfect gas such that the specific heat ratio $\gamma = {C_p}/{C_v}$ is kept constant. However γ is always a function of temperature, leading to the adoption of the iterative procedure to get localized Mach number using

$$\frac{p_{pitot}}{p_{static}} = \frac{\left[\frac{(\gamma+1)}{2}{M_i}^2\right]^{\gamma/\gamma-1}}{\left[\frac{2\gamma{M_i}^2-(\gamma-1)}{\gamma+1}\right]^{1/\gamma-1}} \qquad 3\text{-}28.$$

Pitot tubes and the wall mounted pressure probes enable us to evaluate the exhaust Mach number without depending upon the energy losses due to flow inside the engine. Mach number can be evaluated using the following correlation from the pressure

measurements using the following correlation. It must be emphasized that this relation is valid only for supersonic flows and assumes a normal shock wave present just in front of pitot tube.

3.5.1.3 RAYLEIGH FLOW

For incomplete combustion in the rocket combustion chamber, the engine exhaust might contains some amount of unburnt fuel that could lead to a chemical reaction when it comes in the vicinity if the pitot tube as the localized pressure and temperature is raised due to the presence of pitot tube. This causes a strong shock wave and a stationary flow point with the reaction of the remaining unburnt fuel. This alters the measurements of the pitot tube as the pressure is altered due to the shock wave present right in front of the pitot tube. A physical model was considered in the study in order to take account of this phenomenon as shown in the Figure 3:8.

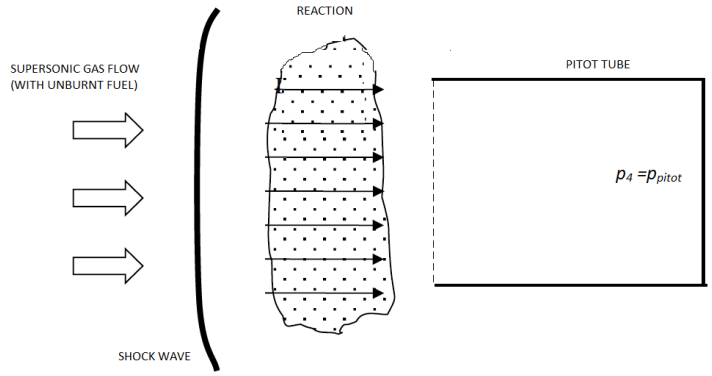

Figure 3:8 Pitot probe with shock wave and reaction ahead

The model states that the gas present in between the pitot tube and the shock wave is considered as Rayleigh flow with the assumptions of frictionless flow with a constant area that allows heat exchange (heat of combustion being the only heat source). The specific heat ratio is assumed to be constant for simplification.

The actual phenomenon occurring is that the supersonic flow with Mach number (M_1) before the shock is being compressed by the normal shock wave that occurs before the pitot tube, yields the subsonic flow (M_2) due to its strong nature followed by a combustion of the unburnt fuel which leading to an increase in the flow velocity before it reaches the pitot tube. It is obvious that for the subsonic flow at the inlet, the final Mach number for Rayleigh flow cannot reach sonic conditions, which also limits the heat transfer to the flow (considering constant mass flow rate).

In order to get the Mach number before the shock wave, an alternative procedure is carried out which involves the evaluation of pitot/static pressure ratio by considering it as the product of pressure ratio across the shock , Rayleigh flow, and the pitot pressure tube .

$$\left(\frac{p_{pitot}}{p_{static}}\right)_{RF} = \frac{p_4}{p_1} = \frac{p_4}{p_3}.\frac{p_3}{p_2}.\frac{p_2}{p_1} \qquad 3\text{-}29$$

Now as the pressure are function of Mach number and the specific heat ratio, all the pressure ratio can be expressed as Mach numbers and specific heat ratio. This simplifies further by assuming sufficient amount of energy being released in the Rayleigh flow in order to make the flow sonic (M_3= 1). Considering isentropic flow, Pitot/Rayleigh flow pressure ratio can be written as :

$$\frac{p_4}{p_3} = \left(\frac{\gamma+1}{2}\right)^{\gamma/\gamma+1} \qquad 3\text{-}30$$

Using the conservation of momentum of the Rayleigh flow, and assuming the final sonic flow, following results are deduced:

$$p_2\left(1+\gamma {M_2}^2\right) = p_3\left(1+\gamma {M_3}^2\right) \qquad 3\text{-}31$$

$$\frac{p_3}{p_2} = \frac{1+\gamma {M_2}^2}{1+\gamma} \qquad 3\text{-}32$$

The normal wave downstream Mach number as a function of freestream velocity is given as:

$${M_2}^2 = \frac{(\gamma-1){M_1}^2+2}{2\gamma {M_1}^2-(\gamma-1)} \qquad 3\text{-}33$$

Substituting the values of M_2, the pressure ratio $\frac{p_3}{p_2}$ becomes

$$\frac{p_3}{p_2} = \frac{1+\gamma\left(\frac{(\gamma-1){M_1}^2+2}{2\gamma {M_1}^2-(\gamma-1)}\right)^2}{1+\gamma} \qquad 3\text{-}34$$

Whereas the pressure ratio across normal shock as a function of freestream Mach number and γ is given as :

$$\frac{p_2}{p_1} = \frac{2\gamma {M_1}^2 - (\gamma - 1)}{\gamma + 1} \qquad 3\text{-}35$$

After the substitution, the pitot/static pressure ratio can be written as:

$$\left(\frac{p_{pitot}}{p_{static}}\right)_{RF} = \left(\frac{\gamma + 1}{2}\right)^{\gamma/\gamma+1} \left[\frac{1 + \gamma\left(\frac{(\gamma - 1){M_1}^2 + 2}{2\gamma {M_1}^2 - (\gamma - 1)}\right)^2}{1 + \gamma}\right] \left[2\gamma {M_1}^2 - (\gamma - 1)\right] \qquad 3\text{-}36$$

Above equation can be used to predict the required flow Mach number for the acceleration of reacting flow till Mach 1 between shock and pitot probe.

When the engine is operated in pure rocket mode, the only component of thrust is the momentum of discharging flow in the axial direction. This requires accurate evaluation of the exhaust Mach number. With the assumption of vacuum at the exit, thrust(considering the average values of M and pressure over the engine exhaust section) is given as

$$F = (\dot{m}v + pA)_{out} = [pA(1 + \gamma M^2)]_{out} \qquad 3\text{-}37$$

3.6 MACH AVERAGING SCHEMES

The evaluation of the engine thrust which can be considered as one of the main important parameter for the Ramjet engine and the rocket motor requires the evaluation of average value of the Mach number at the exhaust if the engine. In order to get a complete understanding of the exhaust flow properties, a set of 11 static wall pressure sensors and 24 pitot probes covering the entire region of the exhaust are implemented in to the exhaust section. Figure 3:9 shows the location of pitot probes and wall pressure probes on the engine exhaust area. With the hypothesis of uniform static pressure along the vertical direction, a plain average can be considered to be valid as the static pressure sensors are uniformly distributed along the span. The pressure ratios (p_{pitot}/p_{static}) provide the local Mach number at the pitot probe location. Linear interpolation between values from neighboring monitoring locations is utilized to obtain localized static pressure at each pressure location. In order to evaluate average Mach number at the exhaust, various schemes can be utilized, which give significantly different results and are discussed below.

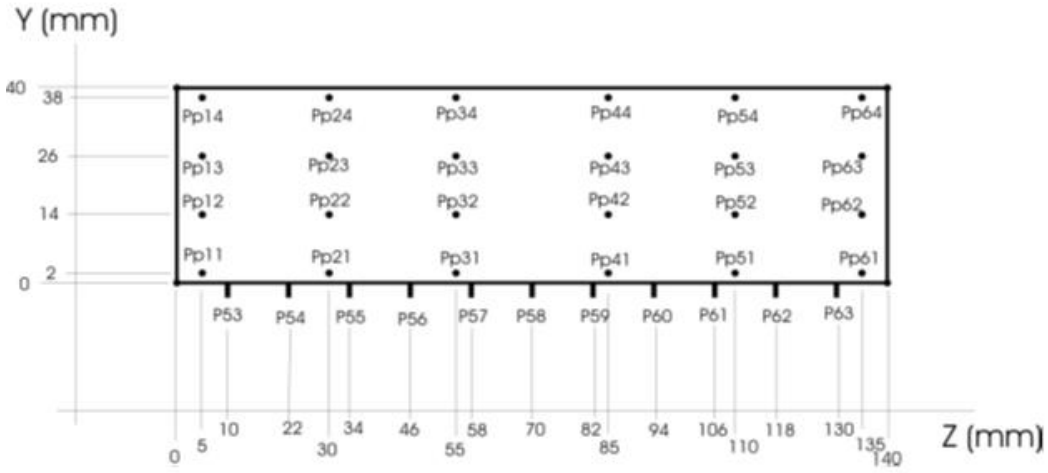

*Figure 3:9 Static wall mounted Pressure sensors and Pitot probes at the Engine exhaust section**

**PpXX = pitot probes, PXX = wall pressure sensors*

3.6.1 SCHEME 1- IMAP=-1

This scheme is the simplest, involving a plain average of the 24 values from pitot locations.

3.6.2 SCHEME 2- IMAP=0

This involves the division of exhaust area in to 35 equal rectangular regions and computing of the weighted average utilizing a specific scheme that is shown in the Figure

3:10. Division is done in a way that vertex of each region coincides with pitot probe location (location with known Mach number) or lays on the wall with M=0.

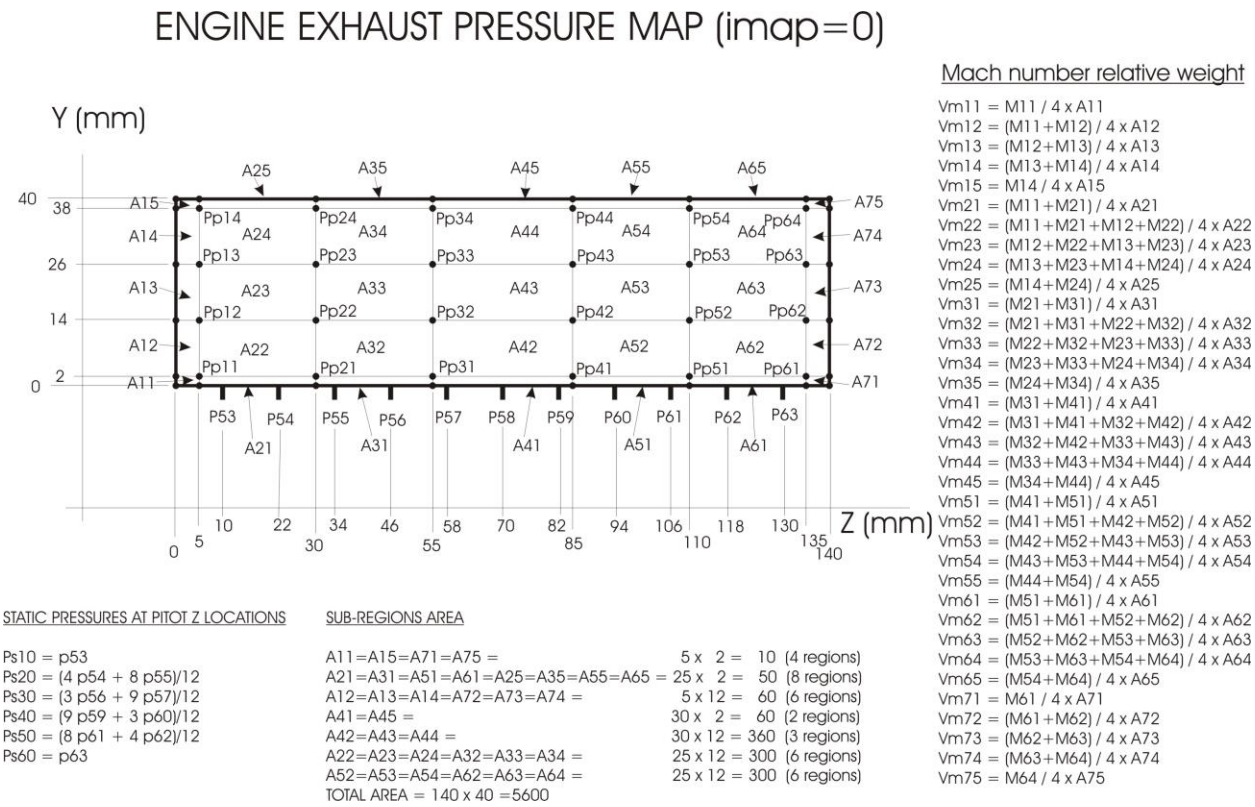

Figure 3:10 Averaging scheme IMAP=0 involving weighted average of the Mach number at the engine exhaust section

In each region, Average of the values at four vertices which give the associated Mach number $\mathbb{M}_{i,j}$ and the relative associated are $A_{i,j}$ with respect to the total exhaust area, $A_{tot.}$ is given in the equation 3.38.

$$\mathbb{M}_{out,0} = \frac{\sum_{i=1,j=1}^{i=7,j=5} M_{i,j} A_{i,j}}{A_{out}} \qquad 3\text{-}38$$

3.6.3 SCHEME 3-IMAP=1

This structure divides the exhaust region into 24 sub-regions and the weighted average is calculated using the scheme shown in Figure 3:11. Regions are not defined on geometrical basis but on the basis of measured Mach number. The Mach number close to the walls gives the thickness of boundary layer(BL) with the assumption that Mach on wall is zero, whereas the external side of BL, outer Mach reaches the value of the nearest monitoring location. Outer Mach numbers on the four sides of the exhaust section considering the scheme in Figure 3:11 are given.

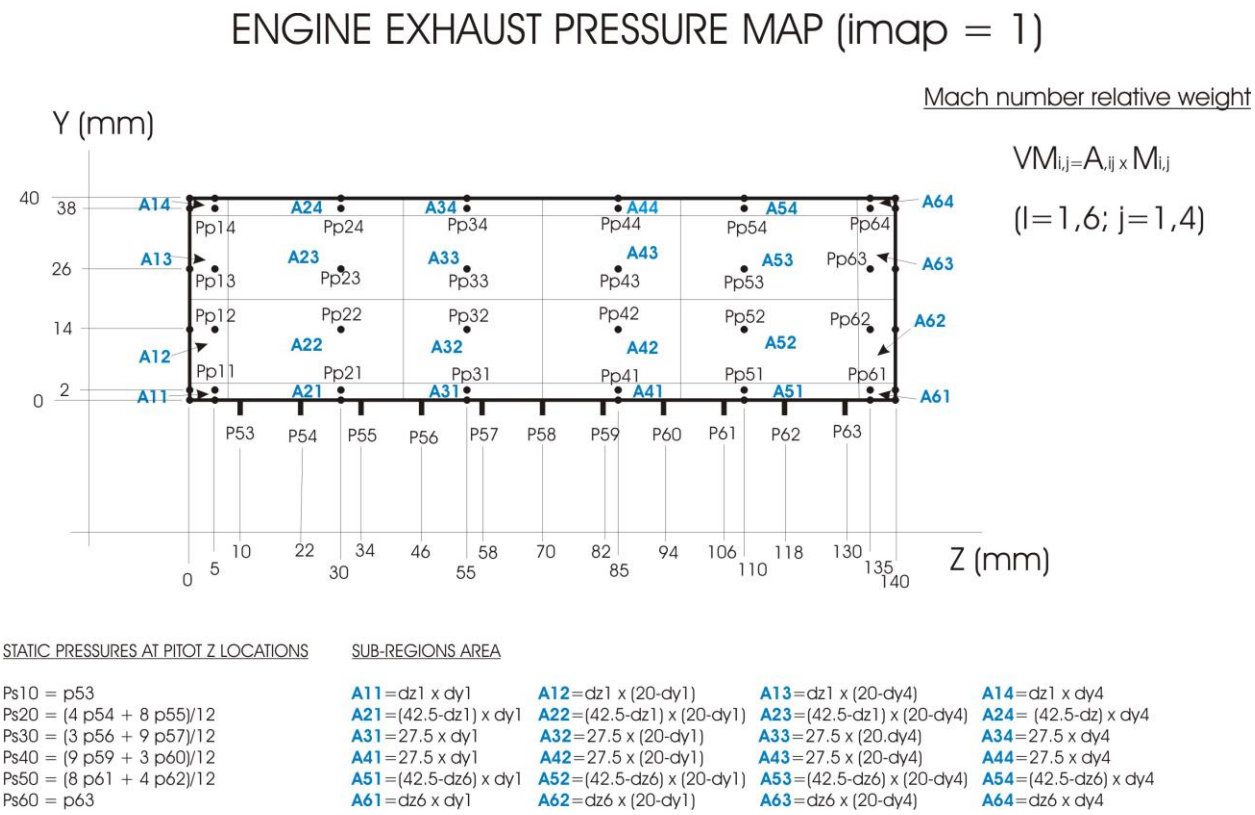

Figure 3:11 Averaging scheme IMAP=1 involving weighted average of the Mach number at the engine exhaust section

The exit Mach numbers on the considered rectangular section can be evaluated using the equations 3-39, 3-40, 3-41 & 3.42.

$$\overline{M}_{e,left} = 0.5\left(M_{2,2} + M_{2.3}\right) \qquad 3\text{-}39$$

$$\overline{M}_{e,top} = 0.25\left(M_{3,3} + M_{2.3} + M_{4.3} + M_{5.3}\right) \qquad 3\text{-}40$$

$$\bar{M}_{e,right} = 0.5\left(M_{5,2} + M_{5.3}\right) \qquad 3\text{-}41$$

$$\bar{M}_{e,bottom} = 0.25\left(M_{2,2} + M_{3,2} + M_{4,2} + M_{5,2}\right) \qquad 3\text{-}42$$

The generic distance between pitot probe and the wall is given by $\delta_{i,j}$, the thickness of generic boundary region is given by equation 3-43.

$$\Delta_{i,j} = \delta_{i,j}\frac{\bar{M}_e}{M_{i,j}} \qquad 3\text{-}43$$

Mach number associated to the boundaries are the averages on the corners, considering the Walls with Mach 0 and Mach on the internal corners as same as that of nearest pitot probe. After defining all the Mach numbers, average Mach number on the exhaust section is:

$$\bar{M}_{out,1} = \frac{\sum_{i=1,j=1}^{i=6,j=4} M_{i,j}A_{i,j}}{A_{out}} \qquad 3\text{-}44$$

Another possible way to compute the average Mach number at the exhaust section leading to evaluation of exhaust gas momentum and thrust is given as:

$$\bar{M}_{out,F} = \left(\frac{\sum_{i=1}^{ALL\ REGIONS} {M_i}^2 A_i}{A_{out}}\right)^{1/2} \qquad 3\text{-}45$$

The above equation 3-45 leads to the value of momentum, that is quite similar to the value obtained from the sum of momentum of stream-tubes associated to all sub-regions defined into the exhaust area, when average value on the whole section is used instead of local static pressure.

3.7 FORTRAN SOURCE CODE

A specially devised code of FORTRAN language was used in order to evaluate the different parameters, which used the set of data obtained in the form of text files from the sensors during the tests. This code was devised in a way to give the output files with the time histories of Pressures, Temperatures, Thrust, Specific Impulse, Mach numbers at several locations (based on the pressure readings at the corresponding locations), averaged Mach numbers (according to the selected scheme) and other parameters like Heat transfer rate, ER, combustion efficiencies of rocket and RAMJET (which is zero because of no fuel injection in the ramjet combustion chamber), etc. These parameters are discussed in detail in the chapter 4. The code was provided by Dr. Giulio Riva who is the Co-advisor for this thesis & a leading researcher at CNR-IENI-Milano.

4 CHAPTER 4

4.1 RESULTS FROM TESTS WITH AND WITHOUT CHEMICAL REACTION

The test facility was set up according to the geometrical configuration described in detail in the Chapter 3. Hydrogen and oxygen being used as fuel and oxidizer respectively were fed in to the system by using solenoid valves and the tests were performed under several operating conditions. The fuel and oxidizer pressures were varied from 10 bar to 20 bar and the data set was recorded for multiple tests. The table 1 shows the reservoir pressures of hydrogen and oxygen for selected tests(out of all the tests, these were selected to perform calculations) performed using the same configuration. The reservoir pressure of both gases decreased with time as the fuel was injected in the rocket. Rocket only mode did not required the use of the stagnation vessel and the facility nozzle as all the test were performed in nearly vacuum. These tests lasted for a fraction of second during which the reactants were fed in to the rocket and the data acquisition system was able to get the values of pressure and temperature at various locations in the engine. This set of data was then processed using a specially designed FORTRAN code (the procedure is mentioned in section 3.5 in detail) which gave the final results which were plotted using MATLAB plotting tool in order to compare and to understand the results.

TEST	HYDROGEN PRESSURE	OXYGEN PRESSURE	REACTION
Setup 1	10	10	No
Setup 2	10	10	Yes
Setup 3	20	20	No
Setup 4	20	20	Yes

Table 1 The Selected tests from the database to perform calculation

Table 1 shows the two different types of tests, with and without ignition of the fuel. The fuel was fed in a similar pattern in both type of tests but was not burnt in one of them, in order to study the combustion properties and the change in the properties with combustion. The detailed results are discussed in the later sections of this chapter.

4.2 NON REACTION TESTS

Hydrogen & oxygen were fed in to the rocket combustion chamber (Setup 1 & Setup 3) but the spark plugs were not fired in order to get the results without the chemical reaction between the reactants. Such tests were carried out to investigate the amount of Thrust increment during the combustion tests.

It is worth mentioning here that the evaluation of all the parameters is done by assuming quasi-steady approach and the validity of results require the quasi-steady assumption to be met. The test results over the whole test duration (i.e. from 50ms untill 500ms) were evaluated and several sharp peaks were seen which typically during the beginning and the end of the reactants flow which were neglected as the system showed transient behavior.

Figure 4:1 shows the **injection pressures** of the reactants during the tests 1 & 3. It is quite clear that the pressure of the reservoir tend to decrease with time as the reactants. The temperature of the rocket chamber remained constant throughout the test (ignoring the transient regions). The figure shows that the complete blow out of the oxygen reservoir occurs at around 300ms and fuel is still supplied later on.

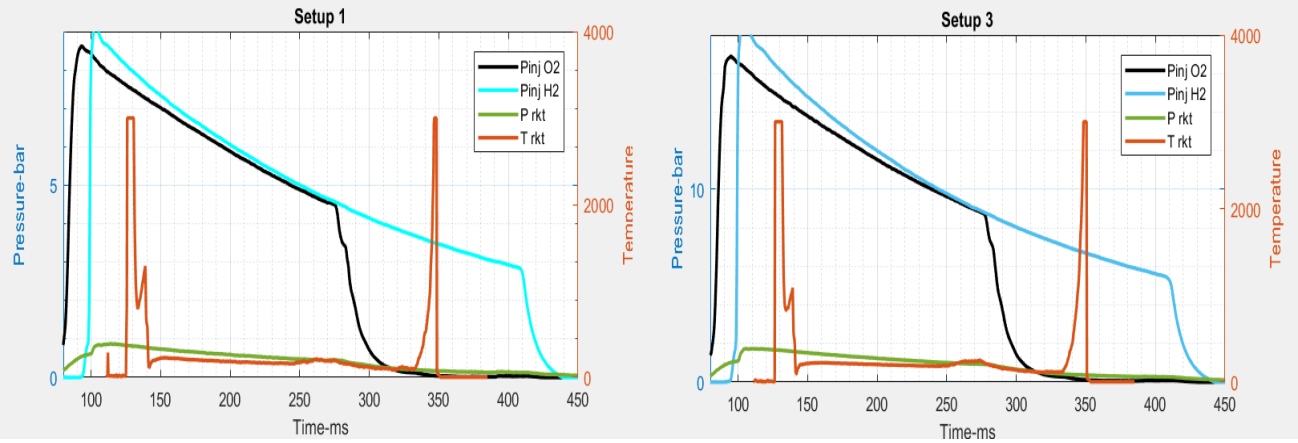

Figure 4:1 Injection pressures of the reactants plotted along with the Pressure & Temperature of Rocket

Figure 4:2 shows the **pressures** at various location inside the engine(figure 3). The pressure at location "O" that is just behind the throat shows the highest pressure, whereas the throat area(minimum cross sectional area) "Q" pressure is slightly lower which supports the fact the flow in the engine is subsonic (as for flow to be supersonic, the highest pressure must be at the throat).

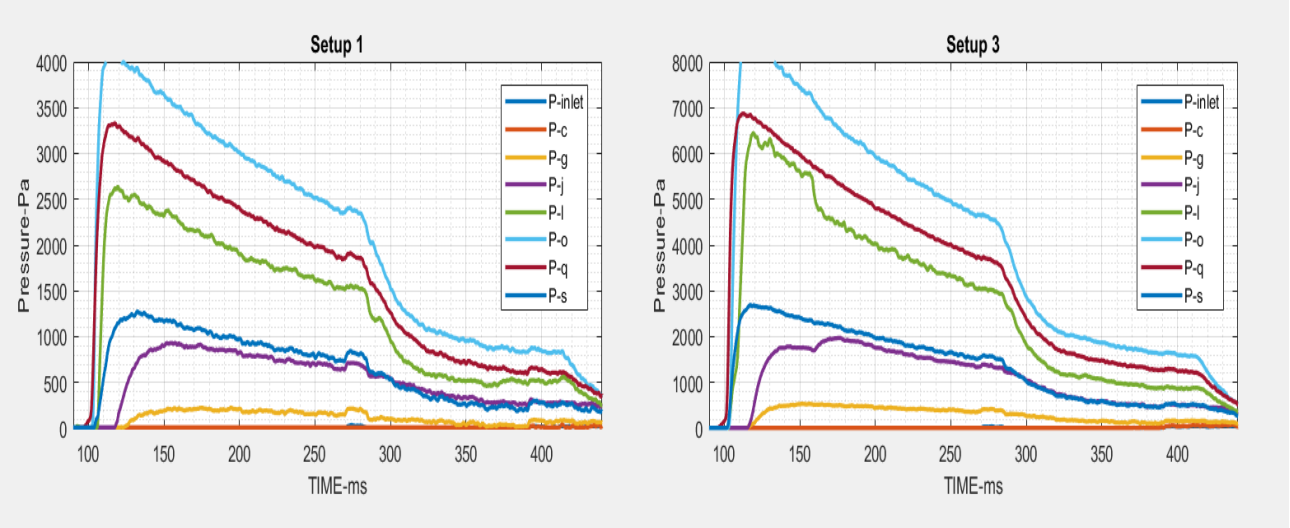

Figure 4:2 Time history of Pressure measurement at different locations

Static temperatures at several location inside the engine are shown in Figure 4:3. The temperatures are seen decreasing throughout the non-reaction tests except during the transient period in which sharp rise in temperature is witnessed (which are not shown in the figure). Due to the assumptions of quasi-steady flow, the sharp peaks are neglected as they show a transient behavior. The decrease in the temperature could be explained as they are initially kept at the room temperature which is due to sudden expansion which causing cooling effect, hence decreasing the temperature. The rocket was kept at vacuum in the beginning while the reactant gases at a positive high pressure.

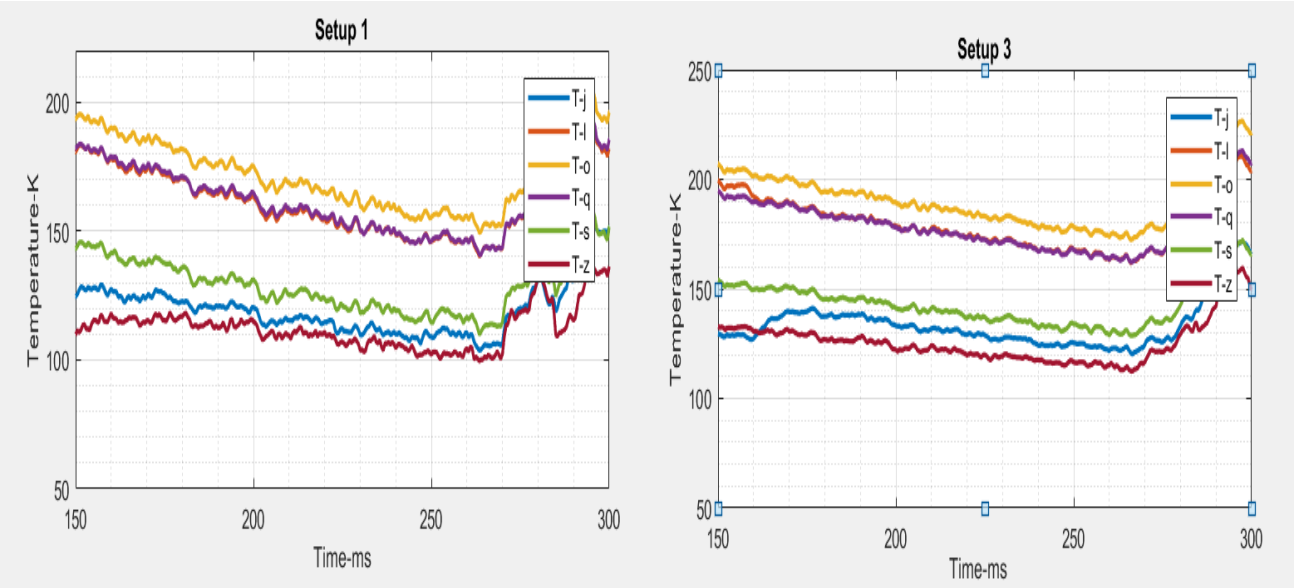

Figure 4:3 Static Temperatures at several locations in the Engine

Thrust is plotted against the time duration of the complete tests in figure 16. The Numerical value of the thrust shows a sudden peak in the beginning that depicts the transient duration, whereas the later part shows quite good resemblance with the load cell thrust curve. The thrust also showed an increase with increase in the reactants injection pressure.

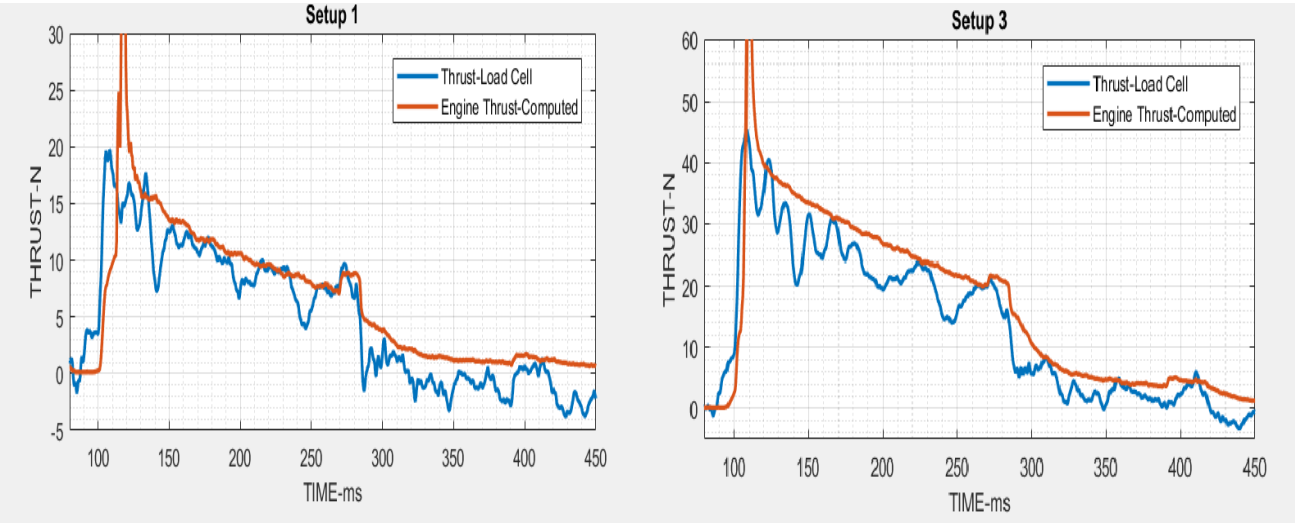

Figure 4:4 Thrust curves for measured and numerical values

Specific impulse shows a constant trend over time for the non-reacting cases as shown in figure 17. At the beginning, there is a sudden increase in the specific impulse at the moment when fuel is fed in to the rocket combustion chamber. It has to be noted here that in this case, Specific impulse is exactly equivalent to the Specific Thrust (Thrust/total mass flow rate).

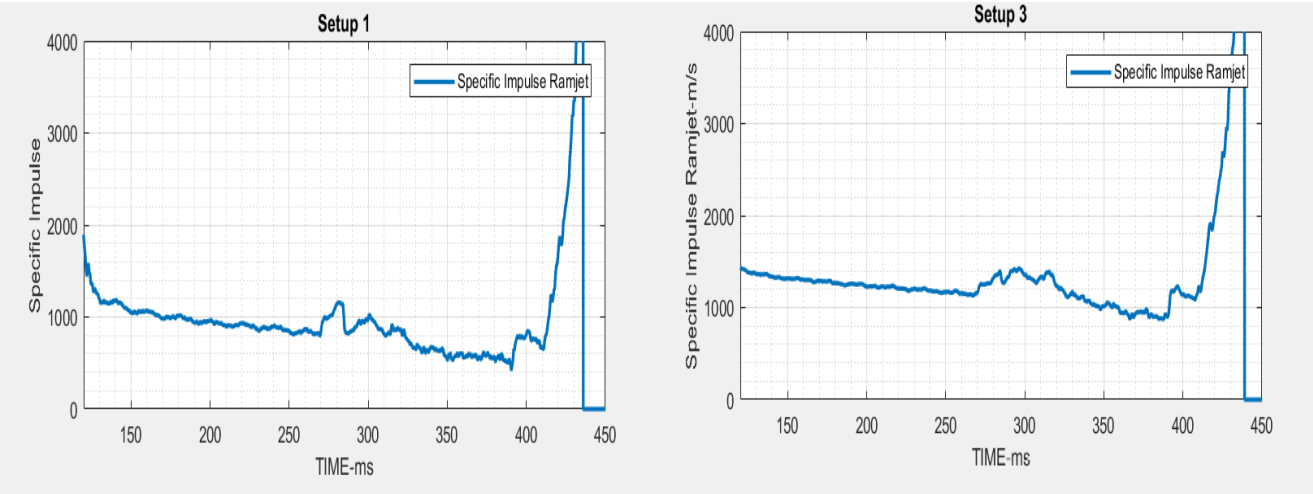

Figure 4:5 Specific Impulse plotted against Time

Figure 4:6 shows Heat Released rate against time . The heat release rate show a negative trend which shows that the heat being absorbed by the rocket walls.

This is due to the fact that a wall heat loss model was not implemented for the rocket combustion chamber. As there is no actual combustion in this case (un-reacting tests), enthalpy balance is utilized to evaluate the heat release rate. The Ramjet combustion chamber can be seen showing shut off during the whole test span.

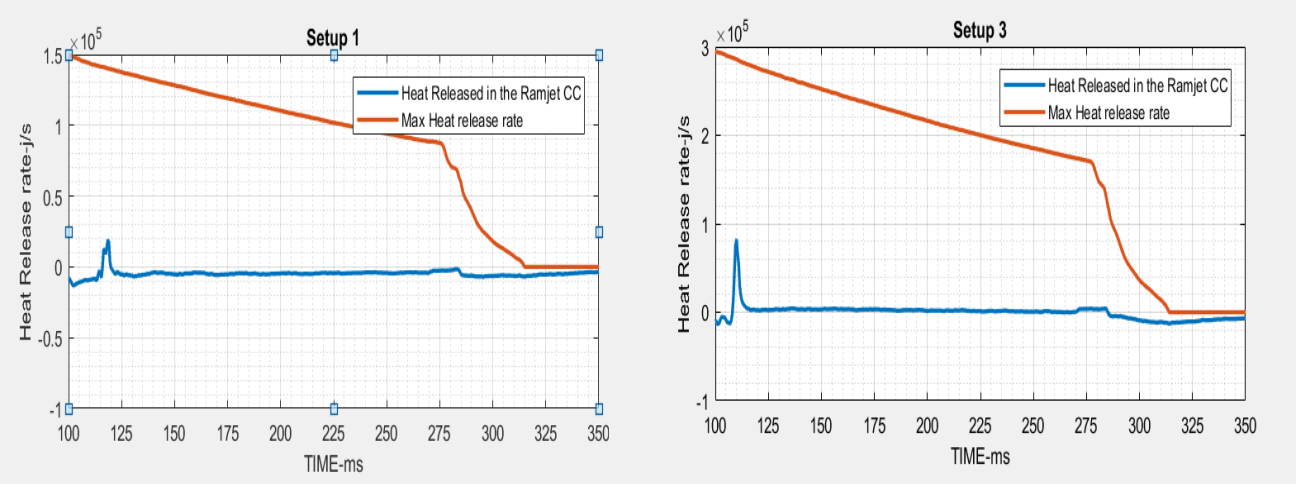

Figure 4:6 Heat Release rate evaluated- Setup 1 & 2

The **Mach number** plotted against time is given in Figure 4:7 Mach number at several locations (IMAP=0)which shows that for non-reacting cases, It is clear that the Mach numbers are subsonic at the throat. However the Mach at "J" & "S" in the beginning show a supersonic behavior. Since the throat section is not having sonic flow, the there is no possibility of supersonic flow in the diverging section of the RAMJET.

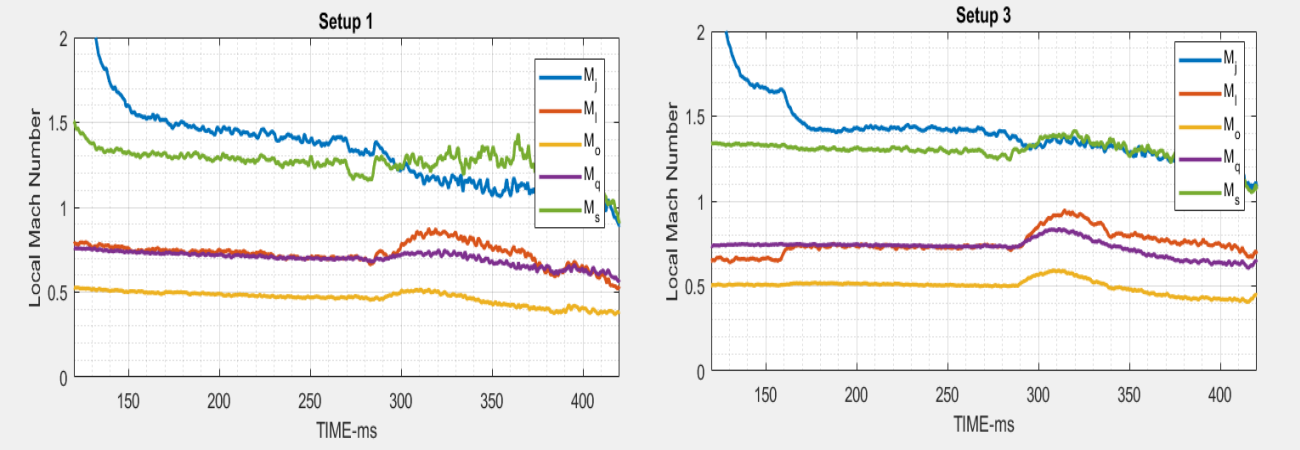

Figure 4:7 Mach number at several locations (IMAP=0)

The pressure sensor at the location **"V"** as mentioned earlier was not considered in these calculations as its values were totally unreliable. Mach number showed an abrupt change when plotted against time, which is totally unrealistic considering the Mach before and after the sensor location "V".

Mach numbers evaluated using the pressure data at the exhaust section (location "Z") is compared with the Mach number evaluated from a very different approach using thermodynamic co-relations, which is mentioned in the graph as Mach-EXHAUST. These two values are also compared with the averaged Mach number at the engine Exhaust using IMAP=0 scheme. The averaged Mach number and the Mach-EXHAUST show an overlapping behavior which can be considered as an embodiment of the validity of the IMAP=0 averaging scheme. Mach number evaluated using the pressure reading from the sensor at the location "Z" shows a transient behavior in the beginning but as it becomes stable, it coincides exactly with the other two curves as shown in Figure 4:8. M_Z showed an abrupt trend in the latter half of the test in the first test (Setup 1) but this problem is seemed to be resolved using a higher injection pressure as seen in the Setup 3 test.

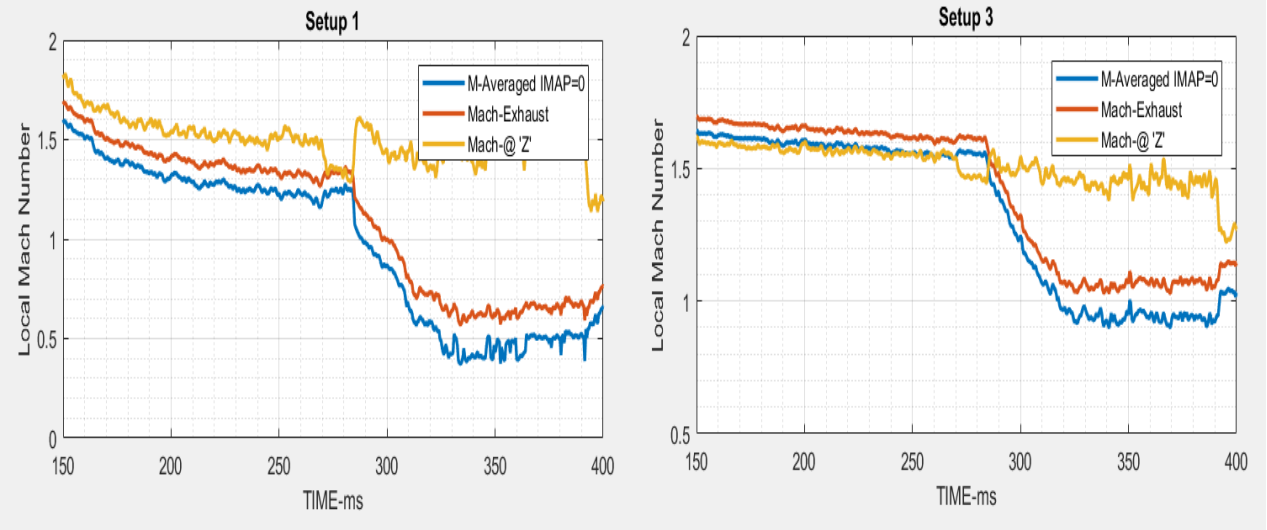

Figure 4:8 Exhaust Mach number evaluated using three different techniques

4.3 RESULTS FROM TESTS WITH COMBUSTION

The facility was operated for a set of operating condition as mentioned in the Table 1. For each setup as mentioned earlier, both the type of test for pure rocket mode were performed i.e. with & without combustion in the rocket combustion chamber. Tests in which there was no combustion served as a reference cases for the tests which were performed with combustion in the rocket combustion chamber under same nominal conditions. Fuel was fed in both the cases in a way to maintain same ER throughout the duration of the tests. Time histories of the parameters(pressure, temperatures & the data from the load cell) were obtained at a frequency of 20kHz with a time bracket of 50ms.

Engine thrust that was computed using the steps shown in chapter 3 based on the measured values of the operating parameters. The computed values of the thrust throughout the duration of the test are done using the IMAP=0 averaging scheme (This scheme gave comparatively similar results with the load cell data than the other two schemes, which is discussed in detail in the chapter 5) . The thrust of the engine decreases with time as shown in Figure 4:9. It can be seen that the highest temperature occurs at the location "Q" corresponding to the throat of the ramjet which is quite realistic.

A comparison between injection pressures of the reactants, rocket average pressure and temperature are given in Figure 4:10. It can be seen that as soon as the oxygen supply is cut off, the temperature curve rises. This leads to the fact that the system is no longer following quasi-steady approach.

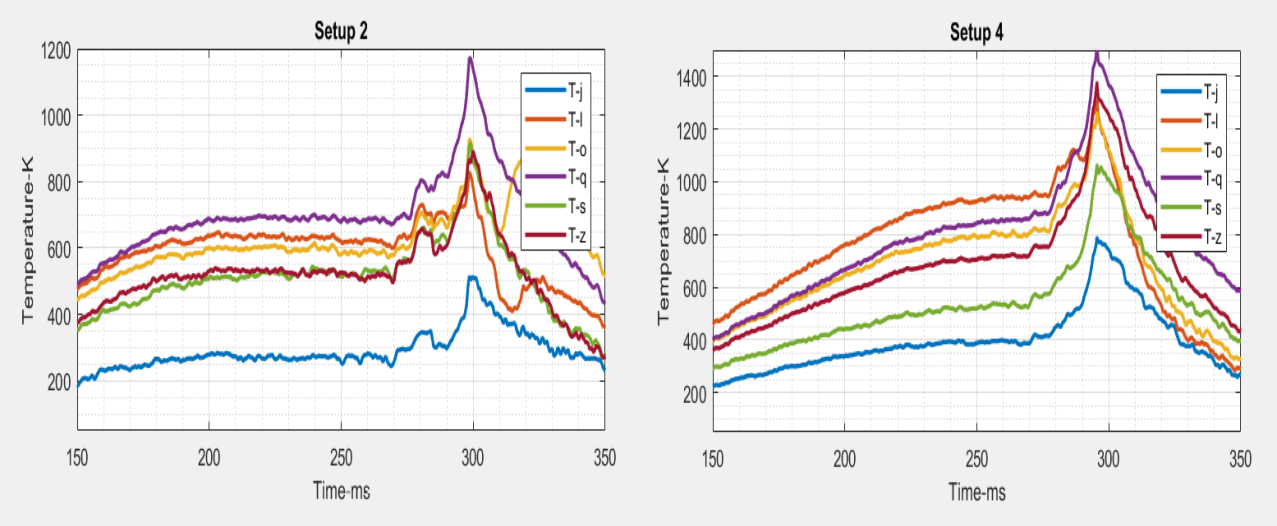

Figure 4:9 Temperature at several locations in the engine during test with combustion

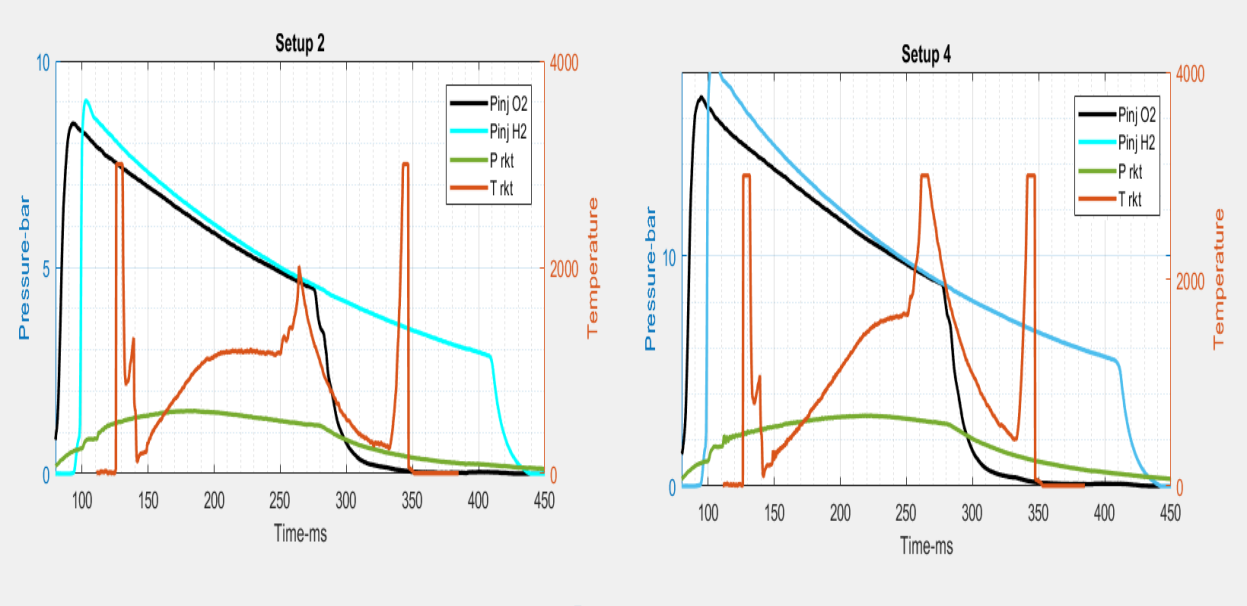

Figure 4:10 Comparison between reactant injection pressures, rocket temperature and pressure

Fuel injection for both the reactants drawn in Figure 4:10 corresponds to exactly the same curves as for the tests without combustion. This leads to the fact that same operating conditions were kept for both types of tests. A sudden increase in the temperature is seen with the oxidizer cut-off as discussed earlier. The rocket pressure shows the increase due to ignition of the fuel in the rocket combustion chamber. Average Static Temperature is also seen increasing due to combustion of the fuel.

The **Engine thrust** computed for non-reacting mixture tests and reacting mixture tests. Comparing the two figures for reacting and non-reacting tests, a considerable increase In the thrust can be observed which is due to the ignition of fuel in the latter tests which leads to the increase in enthalpy of the gases, hence affecting the thrust. This procedure enable us to evaluate the engine un-start thrust and the thrust augmentation by fuel combustion for the complete duration of the test & particularly, during the time period in which the flight conditions are utterly replicated.

Another comparison with the mass fractions of the reactants with the engine thrust is given in Figure 4:12.

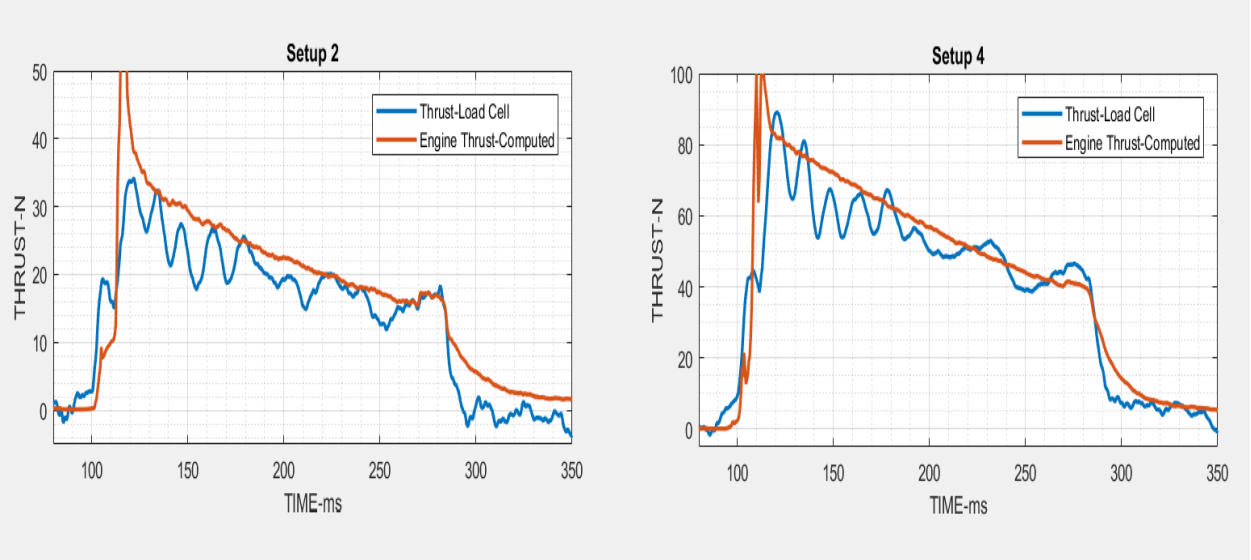

Figure 4:11 Time histories of thrust-Both numerically computed & Load cell data

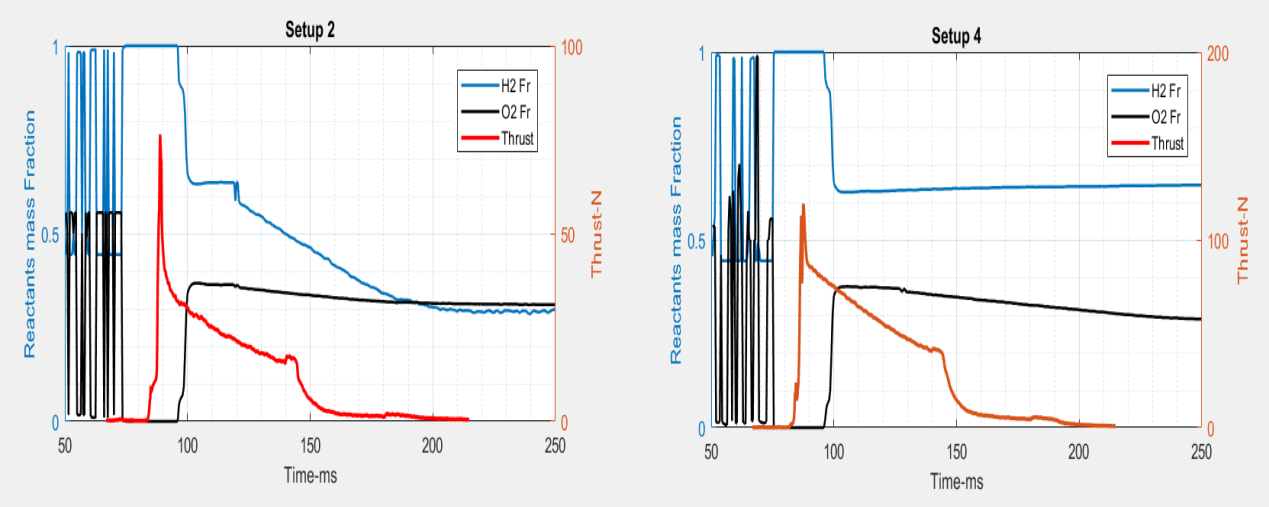

Figure 4:12 Mass fraction of reactants and Thrust curves

Thrust increment is a very important parameter for analyzing of the data set because there could be other independent methods of its evaluation, e.g. Direct Force measurement technique. The combination of the same quantity computed with the help of momentum balance from the pressure and temperature readings obtained from the sensors and the data from the load cell for both the type of tests seem analogous to each other. The thrust increment curves were plotted along the time interval of the test which are averaged on the 50 time window for all the tests is given in Figure 4:13 which shows a significant increase in the engine thrust with combustion of the fuel in the rocket combustion chamber & the increment is even more for higher injection pressures.

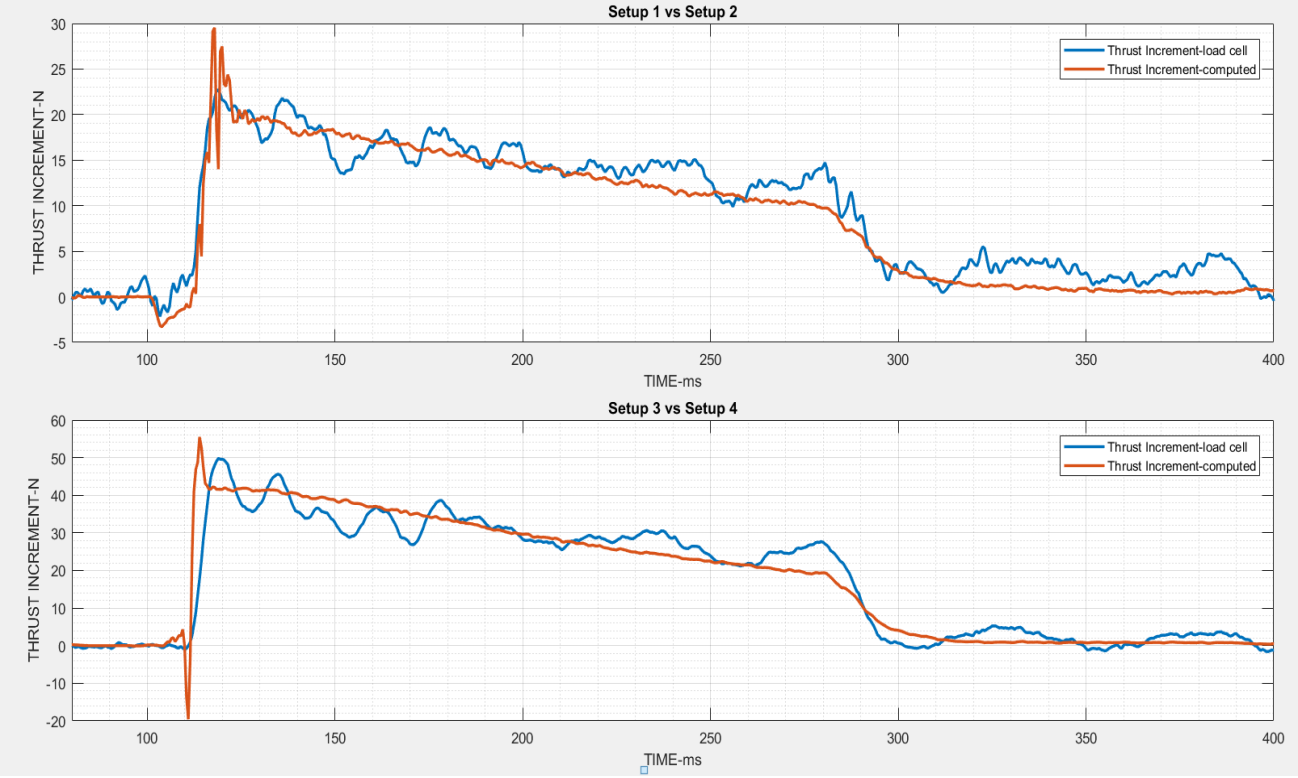

Figure 4:13 Comparison between reaction and non-reaction tests with the similar operating conditions

A size independent parameter **specific impulse** computed using the reactants mass flow rates and the uninstalled thrust is shown in the Figure 4:14. Fuel and oxidizer mass flow rates were evaluated using the injection pressure data (Figure 4:10) with the assumption of sonic flow at the injection ports.

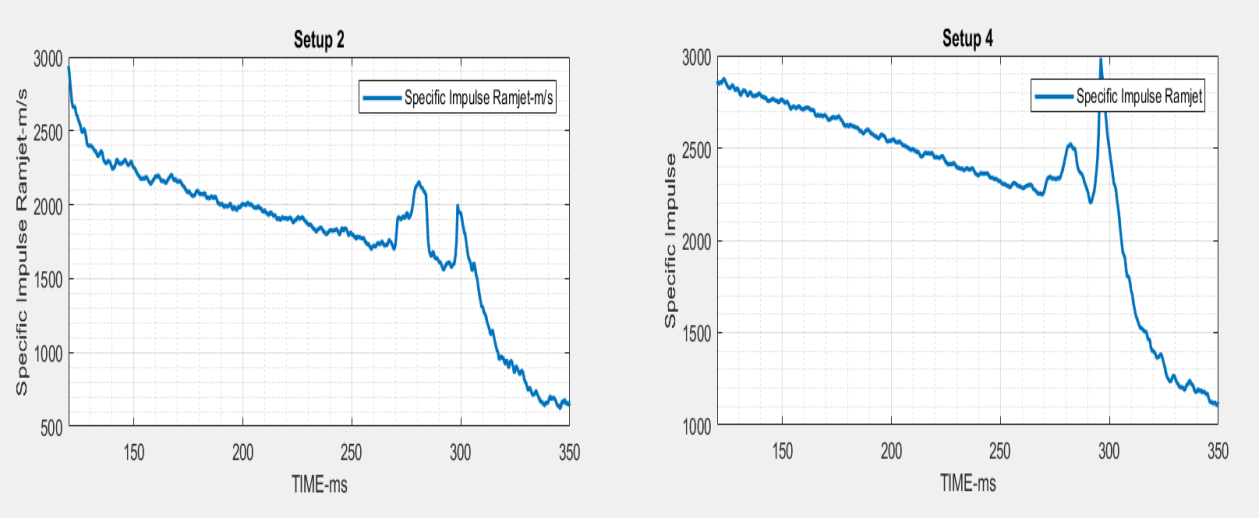

Figure 4:14 Specific Impulse (Axial force divided by total mass flow rate) plotted against time

Other parameters evaluated using the energy conservation equation such as heat release rate, maximum heat release rate computed using enthalpies is given in the following Figure 4:15. Heat release rate can be seen in complete accordance with the one for the non-reacting case. Heat release during the combustion in test setup 4 is exactly the double of the one seen for test setup 2 for which the injection pressure is one half than the other, which shows the relation of the heat release rate with the injection pressure. During the tests with reaction, Ramjet combustion chamber walls are seen to be absorbing a portion of the heat released, by the combustion in rocket combustion chamber.

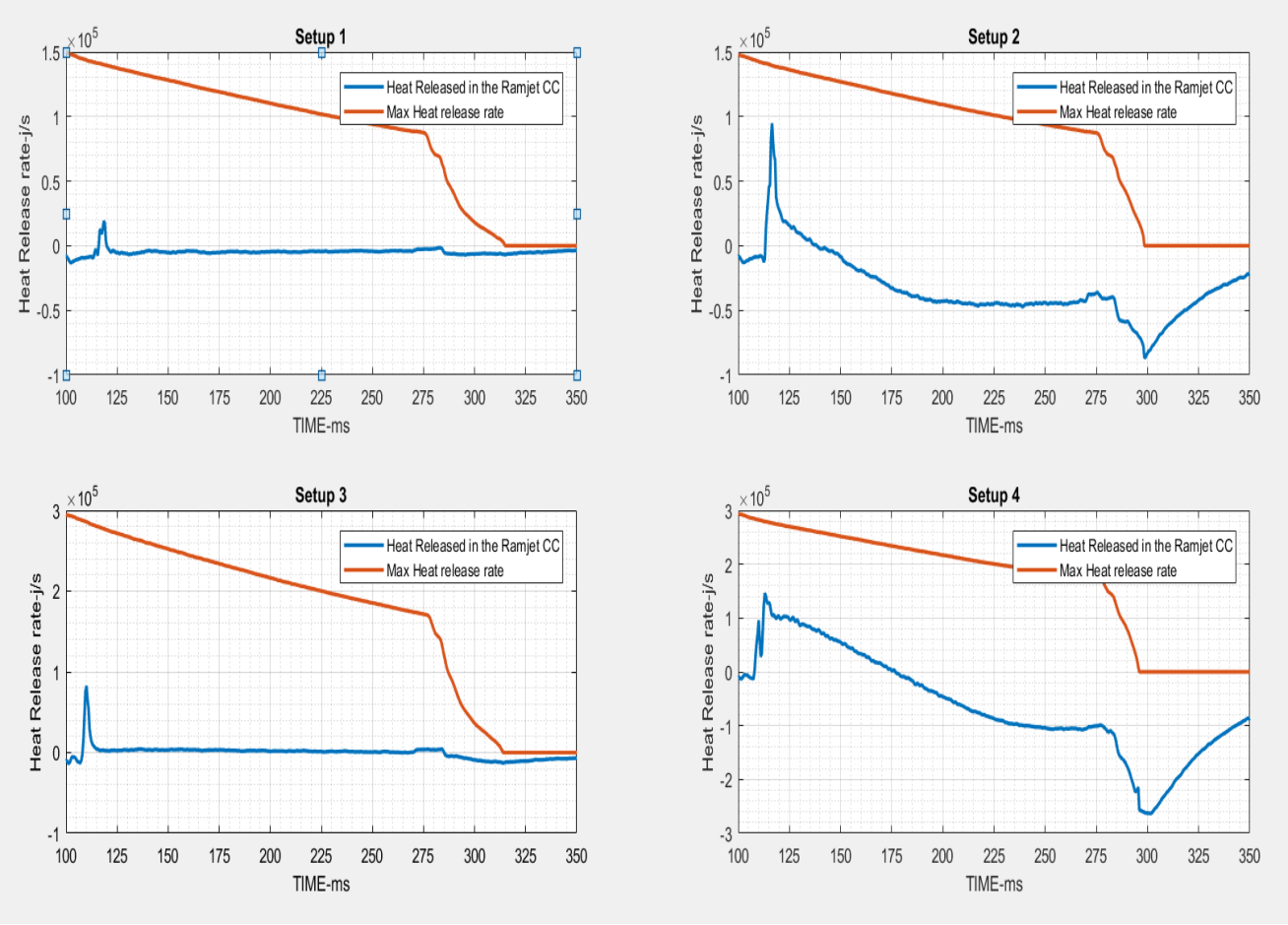

Figure 4:15 Heat release rate due to combustion in rocket & ramjet combustion chamber

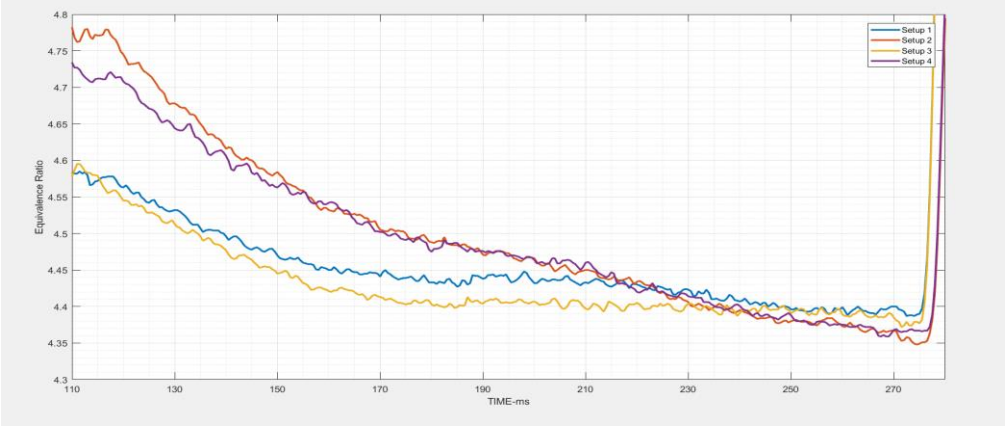

Figure 4:16 Equivalence ratio (ER) plotted against time for all 4 tests

Equivalence ratio showed a constant value(changes are in the range of 1/10th of fraction) during the major portion of the tests, and can be seen constant during the quasi-steady portion. There are some sudden changes in the first 50-75ms but they are neglected considering the developing flow in the engine. A sudden peak is seen at 300ms which is quite unrealistic and is neglected on the basis of the assumptions made at the beginning of the evaluation procedure.

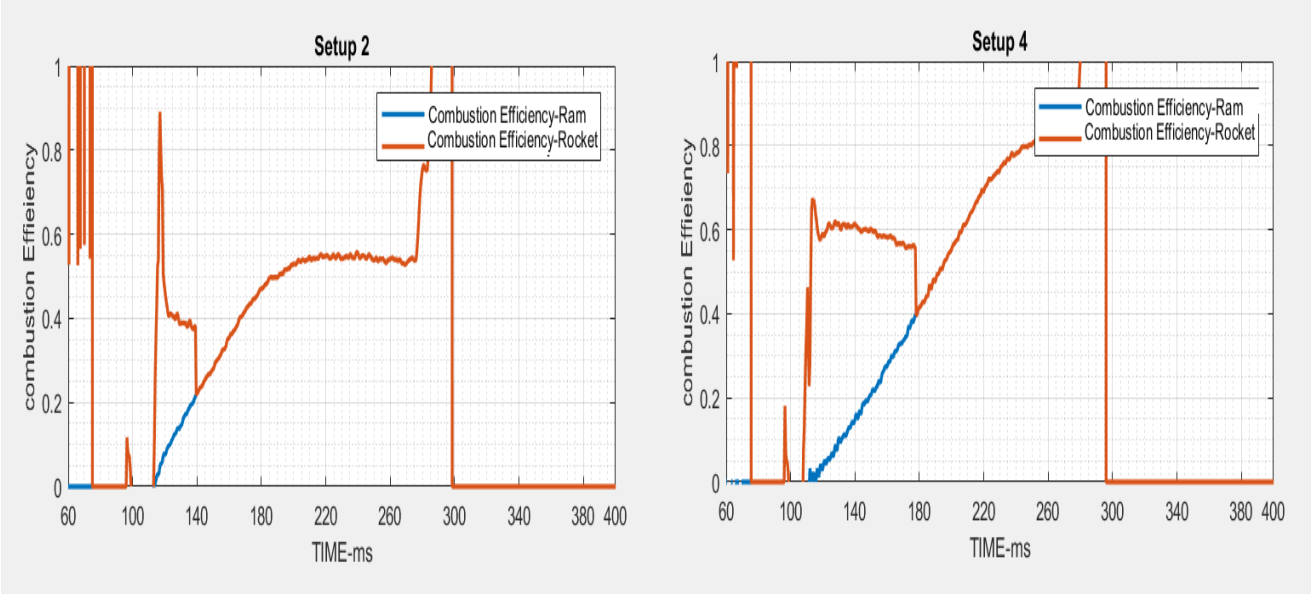

Figure 4:17 A Comparison between the combustion efficiencies

Combustion efficiencies showed an increasing trend with time, and then stabilized near the end of the test. For higher injection pressure, it kept on increasing at a lower rate which refers to the fact that a longer test time is required in order to stabilize the complete combustion.

5 CHAPTER 5

5.1 COMPARISON BETWEEN DIFFERENT MACH AVERAGING SCHEMES

This chapter focuses on the comparison between the parameter obtained using three different kind of averaging schemes for the calculation of Exhaust Mach number as discussed in chapter 3.

Engine Mach number evaluated for all the 4 tests under consideration at various location for all the three schemes are given in the following figures. Figure 5:1 shows a quite good resemblance of the Mach number values for Mach evaluated at the exhaust using an independent technique and the data from the pressure and temperature sensors. Whereas, in the Figure 5:23, the average values of the Mach number (IMAP=1) shows quite conformal trend in the first half of the test until 300ms but later, some back flow is seen from the curve with a negative Mach number. This scheme set could be considered reliable only for the first half of the test, as the corresponding values of the Thrust and specific impulse resulting which are a function of Mach numbers, will lead to wrong values for thrust and specific impulse & other dependent quantities. The plain averaging scheme IMAP=-1 leads to a quite conformal set of curves (Figure 5:32), but in the later half, is shows a slight increase in the averaged Mach number (IMAP=-1) with respect to the $M_{exhaust}$. This problem seemed to quite resolved with the increment of fuel and oxidizer injection pressures.

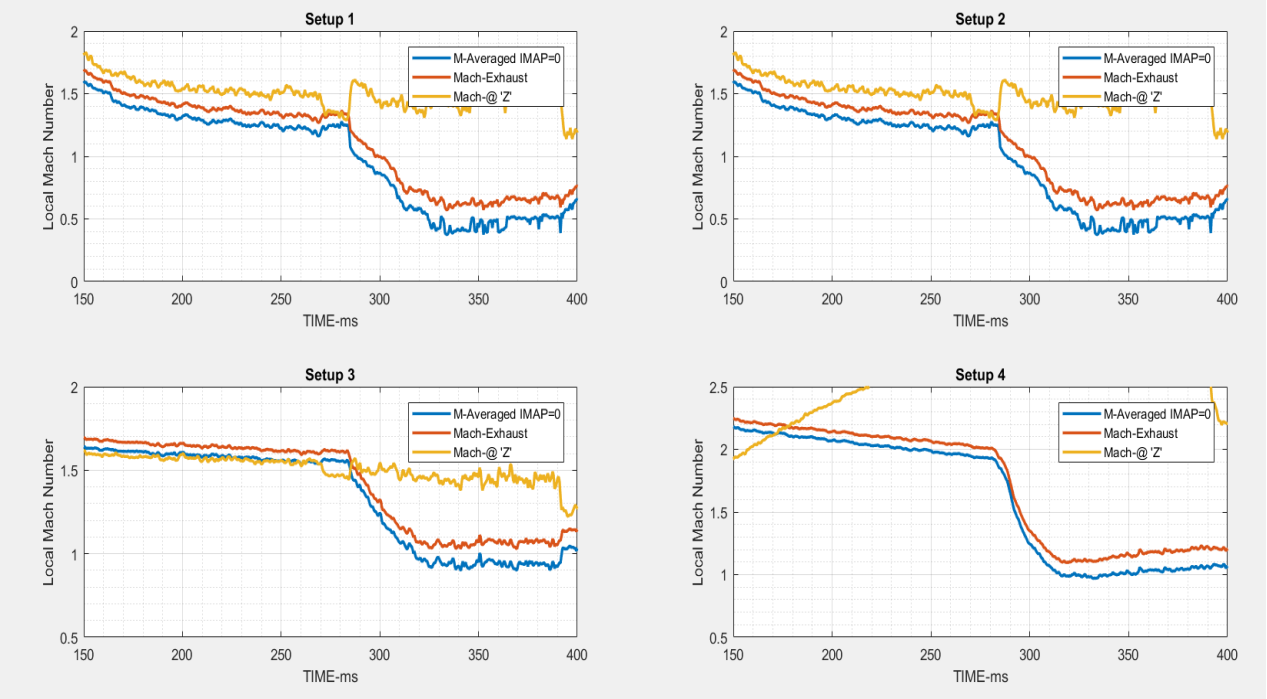

Figure 5:1 Mach number at Exhaust for IMAP=0

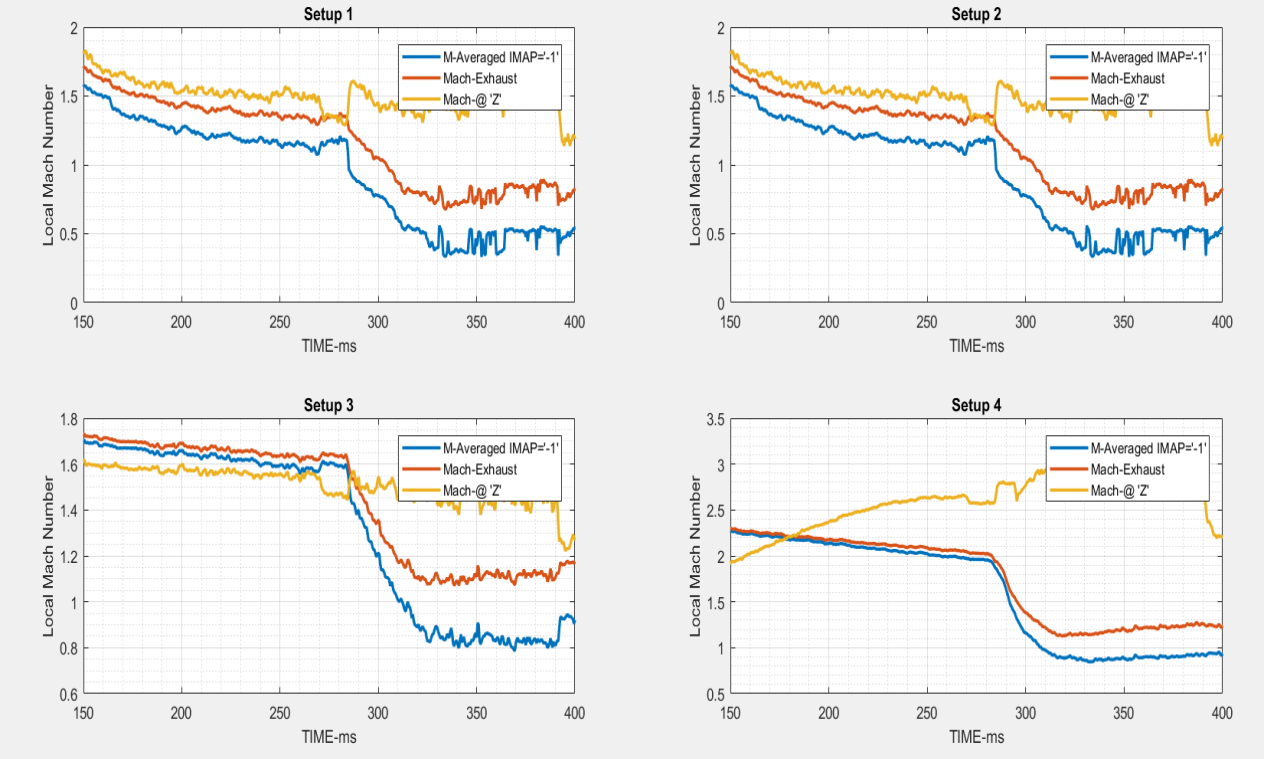

Figure 5:2 Mach number at exhaust IMAP=-1

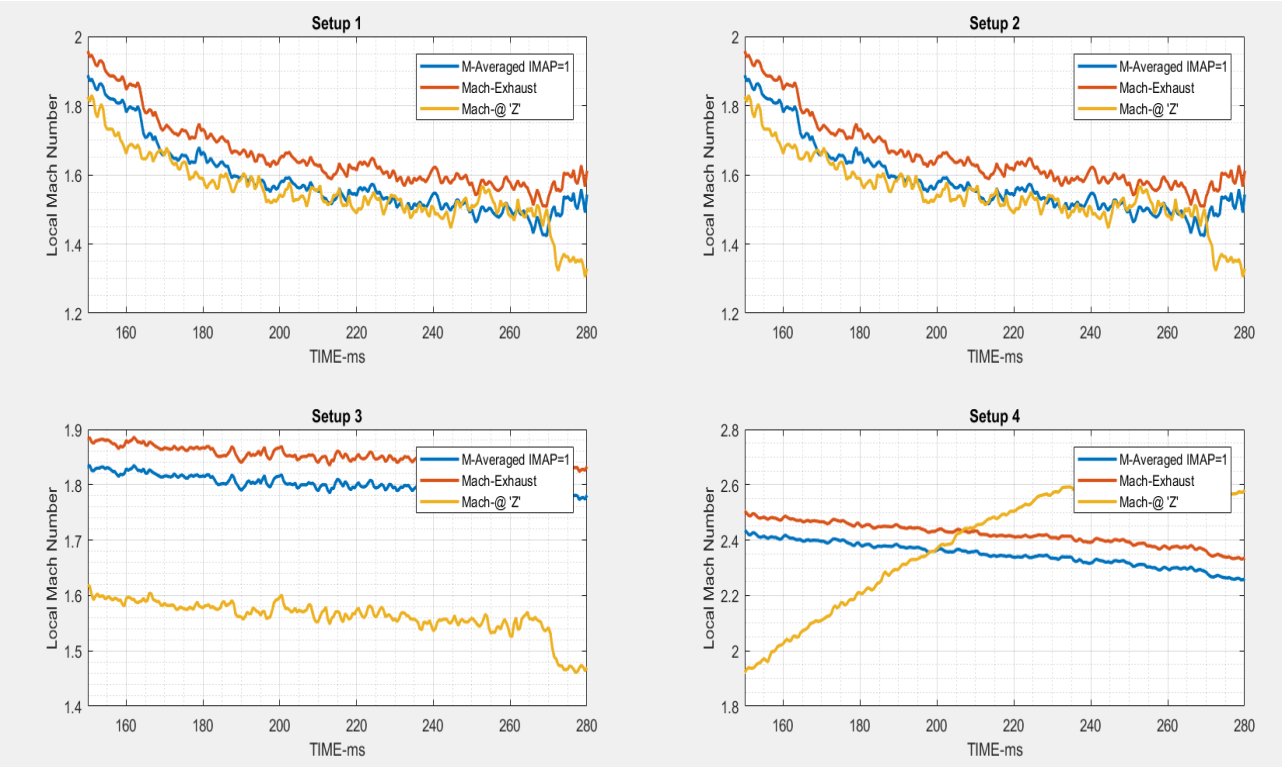

Figure 5:3 Mach number at exhaust IMAP=1

The main important parameter, **Engine thrust** (from the three different schemes) when compared also confirms the validity of the averaging scheme IMAP=0, as the curve seems to be quite similar with the load cell curve. The load cell curve has shown some fluctuations, which is quite typical for a data set from the load cell(Figure 5:4,Figure 5:5,Figure 5:6). The results from IMAP=0 and IMAP=-1 show a similar trend which are quite similar with the load cell curve, but the IMAP=1 scheme yielded a thrust curve which shows quite high values of the engine thrust as compared to the load cell data.

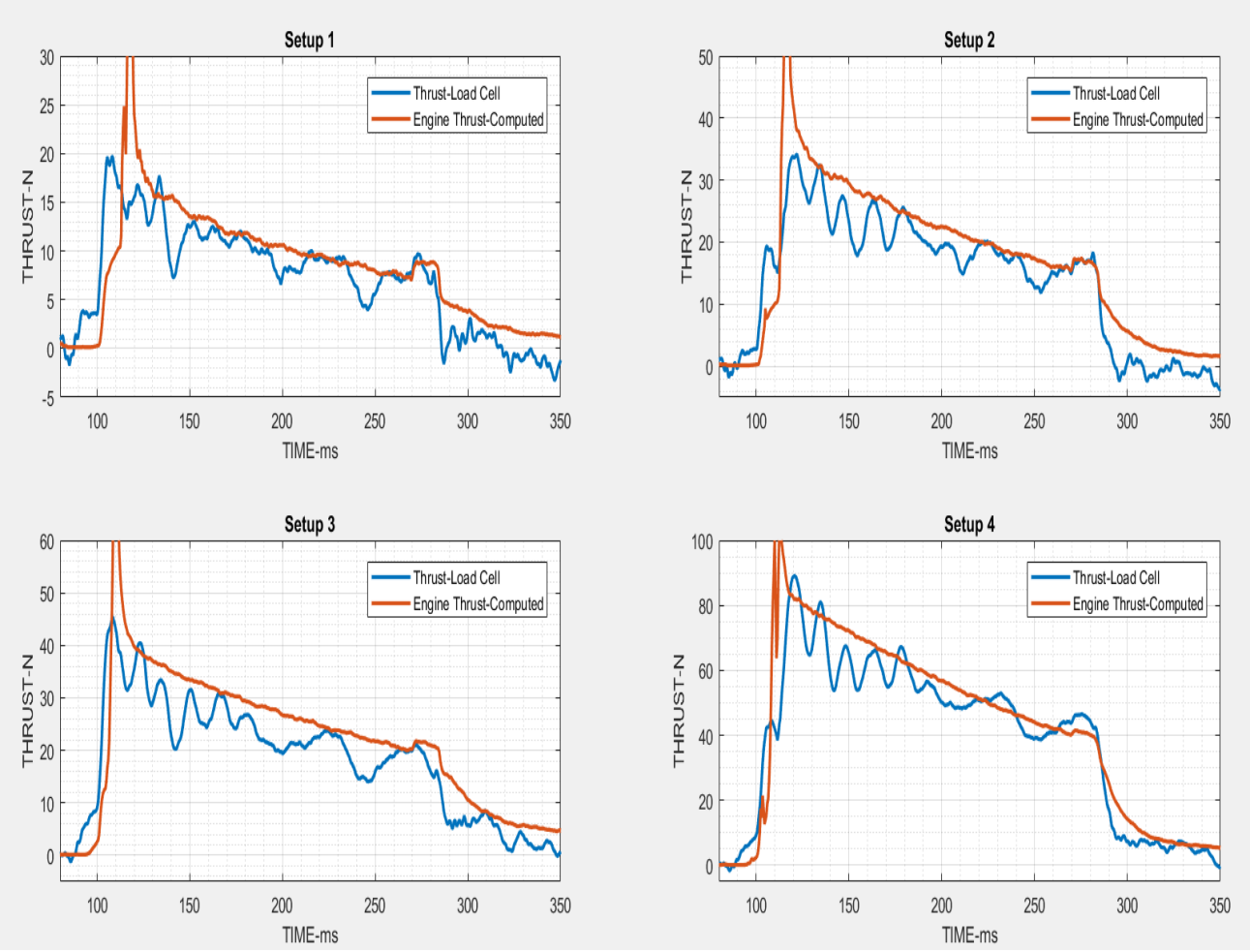

Figure 5:4 Engine Thrust IMAP=0

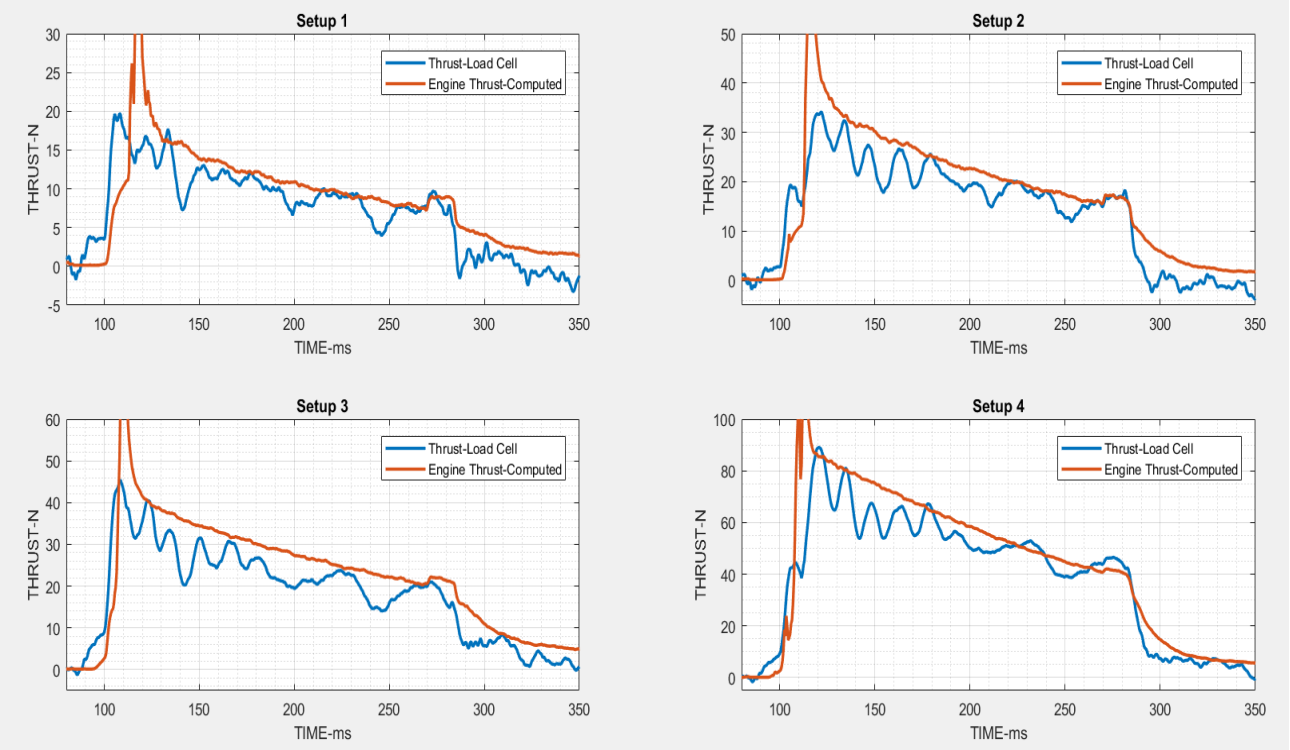

Figure 5:5 Engine Thrust IMAP=-1

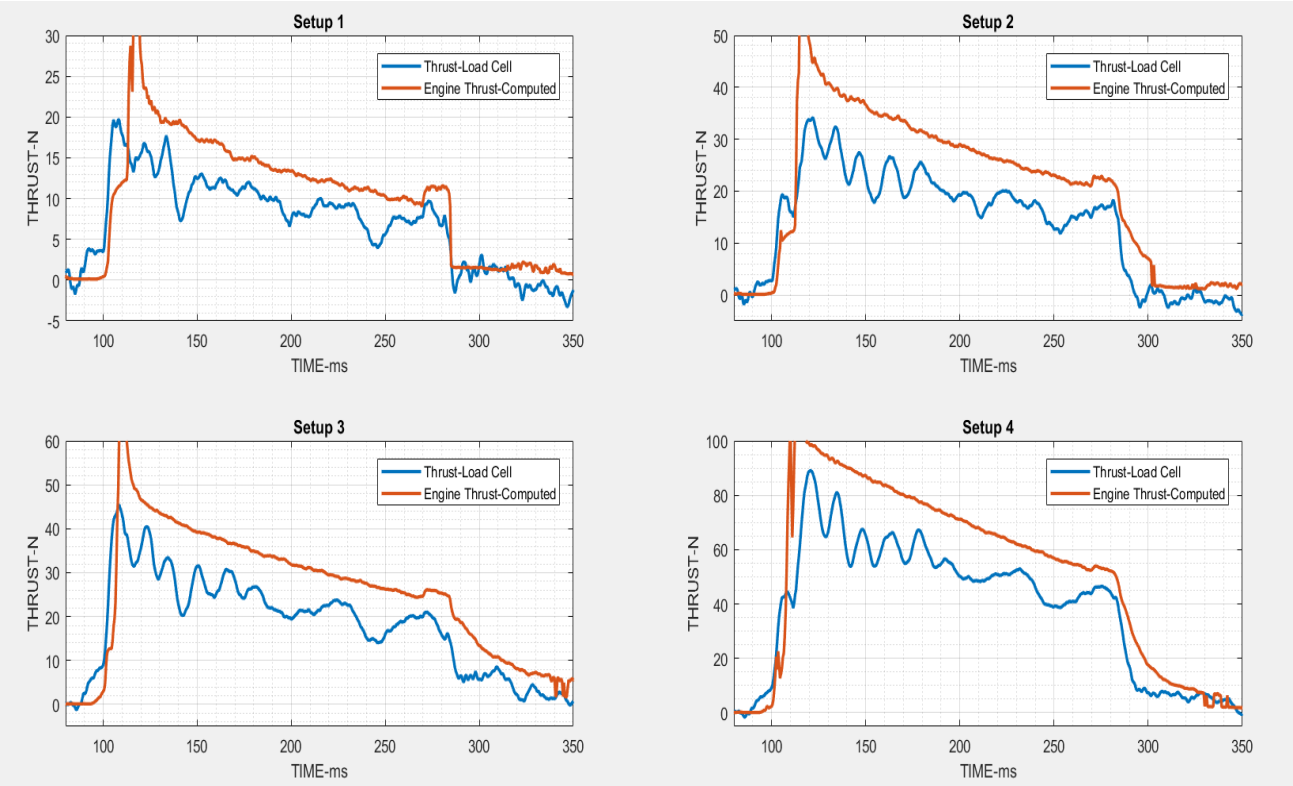

Figure 5:6 Engine Thrust IMAP= 1

5.2 TESTS WITHOUT THROAT AREA

There were several tests performed using the same schematics given in the

Figure 3:2Figure 3:1 but with a slight difference that the throat area was removed that resulted in a configuration with a constantly diverging channel. Tests were run in a similar way as discussed in the chapter 3 section 4. The configuration of such tests is shown in the Figure 5:7.Similar set of the test with & without combustion without throat was selected (Table 2) in order to compare the result with the those discussed in the previous section of chapter 5 and the findings are shown in this section.

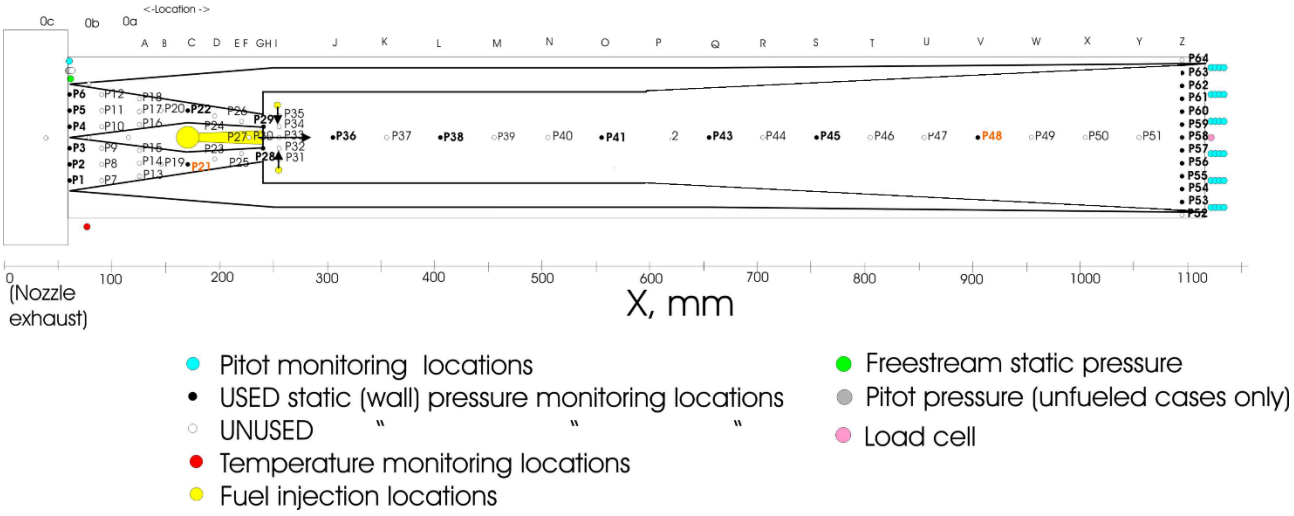

Figure 5:7 Test configuration without Throat

TEST	HYDROGEN PRESSURE	OXYGEN PRESSURE	REACTION
Setup 5	10	10	No
Setup 6	10	10	Yes
Setup 7	20	20	No
Setup 8	20	20	Yes

Table 2 Test configurations for tests without throat

The main interesting results were found by comparing the Mach numbers at the exhaust, Engine Thrust, Thrust increment for tests with combustion & without combustion and Mach numbers at different locations within the ramjet engine. All other parameters were found similar to those mentioned in the previous section for the tests with throat section.

A comparison between Mach numbers at the exhaust of the RAMJET using three independent schemes is given in . This shows that in the first half of the test, the flow is supersonic and as the time increases, it becomes subsonic. This result is quite similar to the result seen in the previous section for the tests with throat (Figure 5:1).

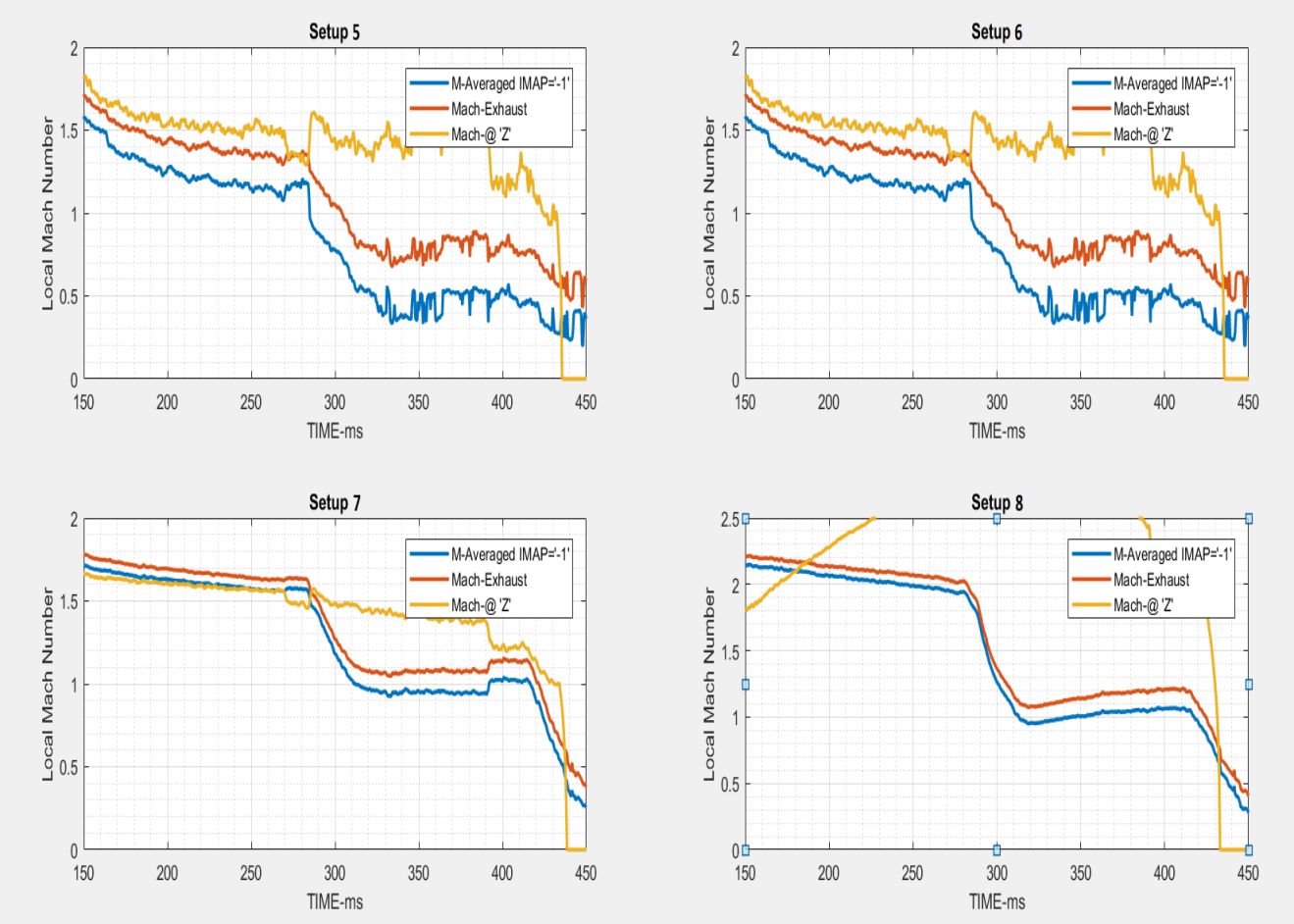

Figure 5:8 Exhaust Mach number evaluated with three different schemes

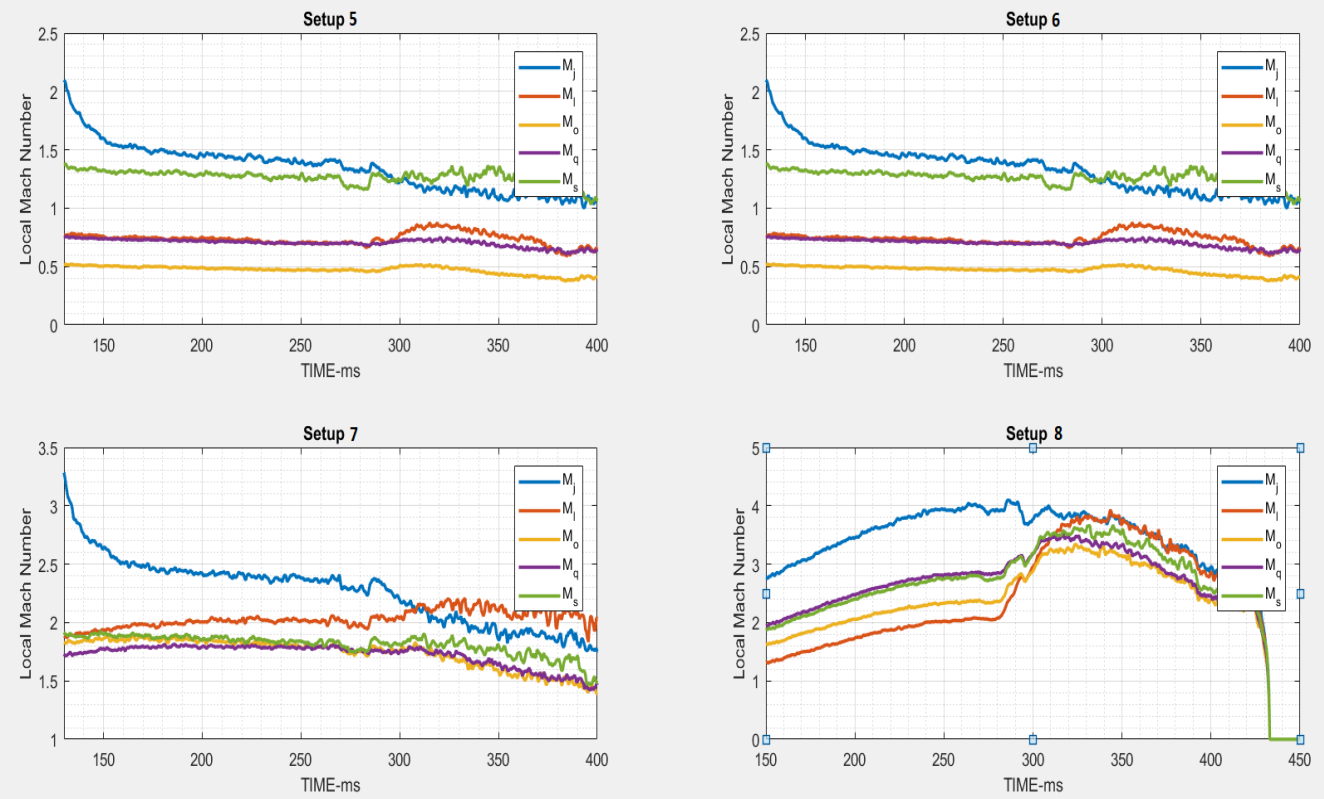

Figure 5:9 Time history of Mach numbers at several location in the ramjet engine

Figure 5:9 shows the Mach numbers at various locations in the engine without throat. For the setup 7 & setup 8, there is a supersonic flow in the engine at all the locations. Whereas, only subsonic flow was seen in engine when operating conditions were kept same and tests were performed with the throat section present.

Another very interesting result observed during the comparison was that the values of thrust for both the configurations are almost the same. Figure 5:9 shows the average values of engine thrust with and without throat section plotted. On comparison, it was found that there was no significant increase in the thrust for the two type of tests (with and without throat).

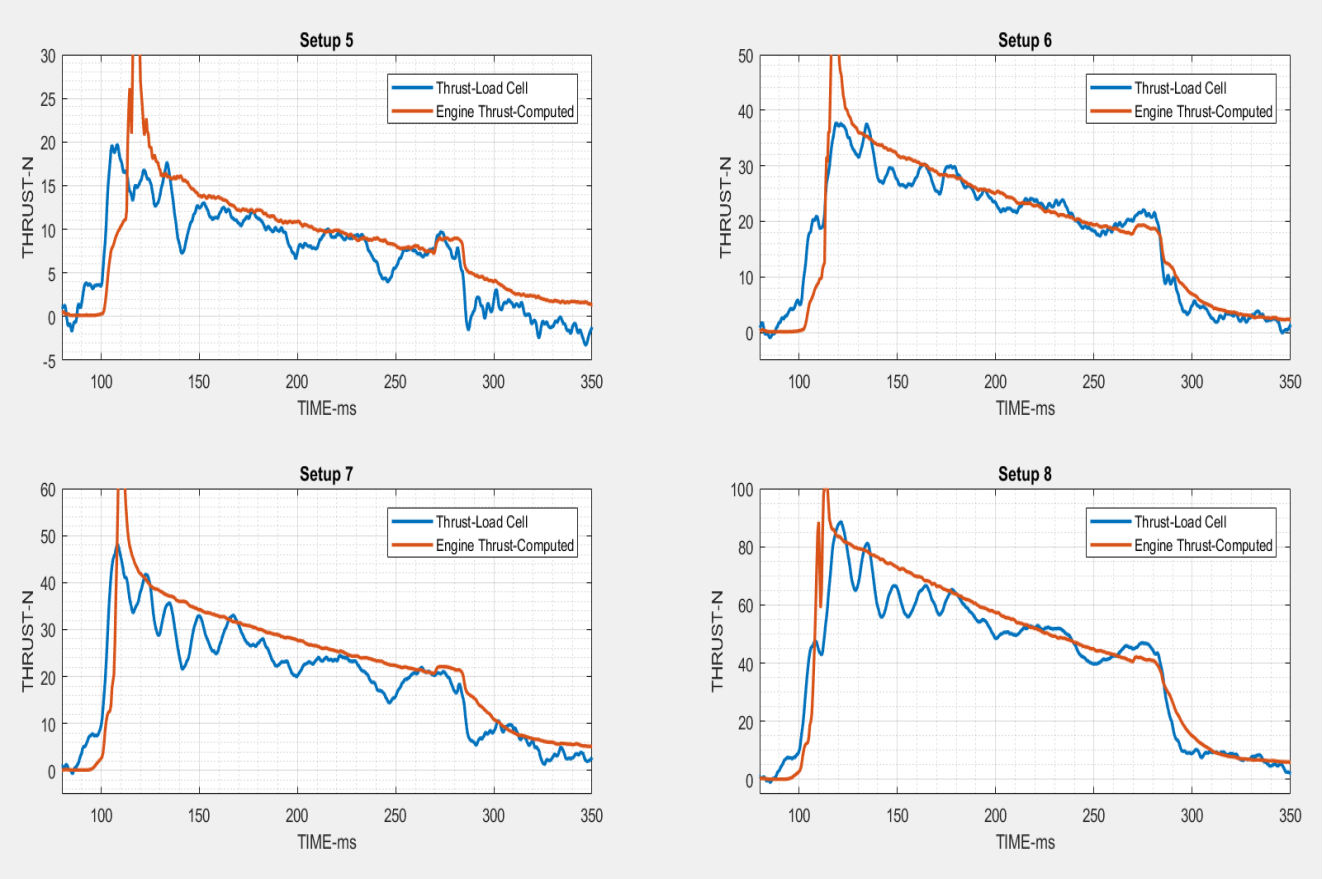

Figure 5:10 Thrust plotted against Time -Without Throat

Figure 5:9 and Figure 5:9 show quite similar values of thrust and thrust increment between the tests with and without combustion, as seen in the previous section for the tests with throat.

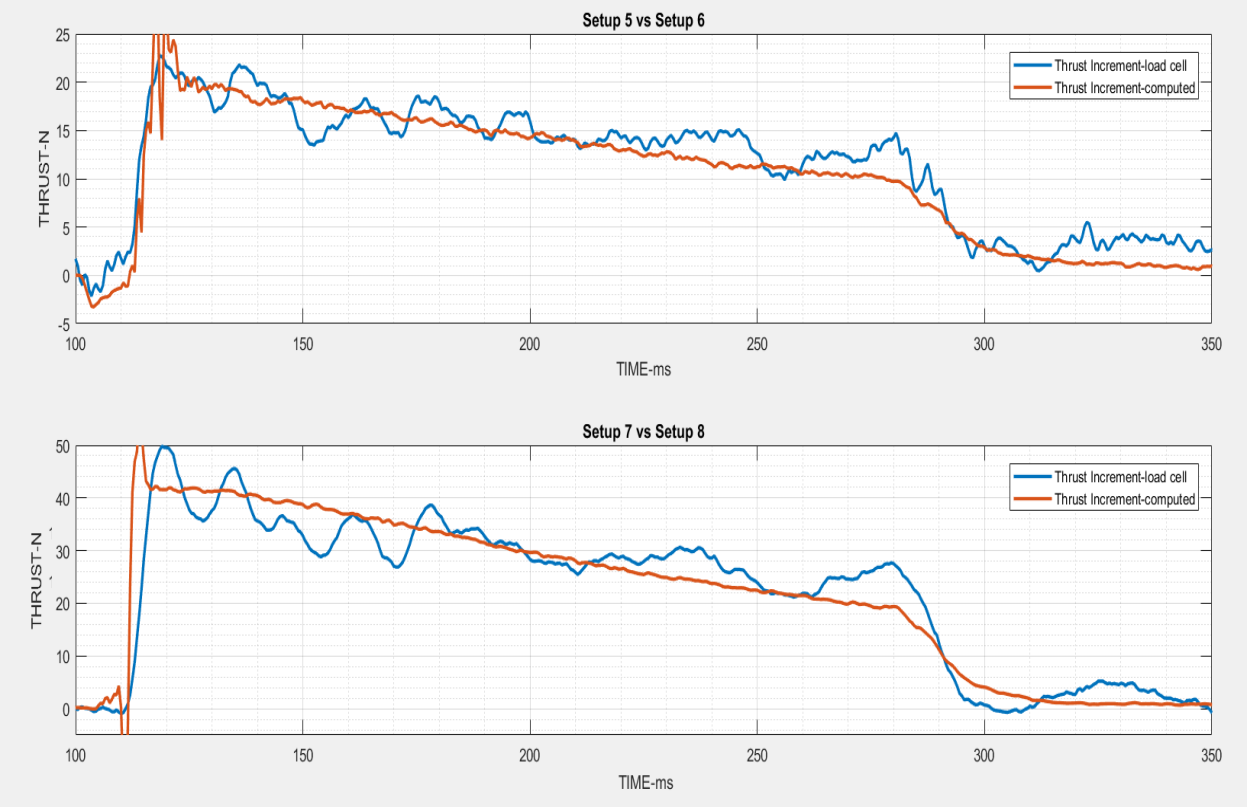

Figure 5:11 Thrust increment-Without Throat

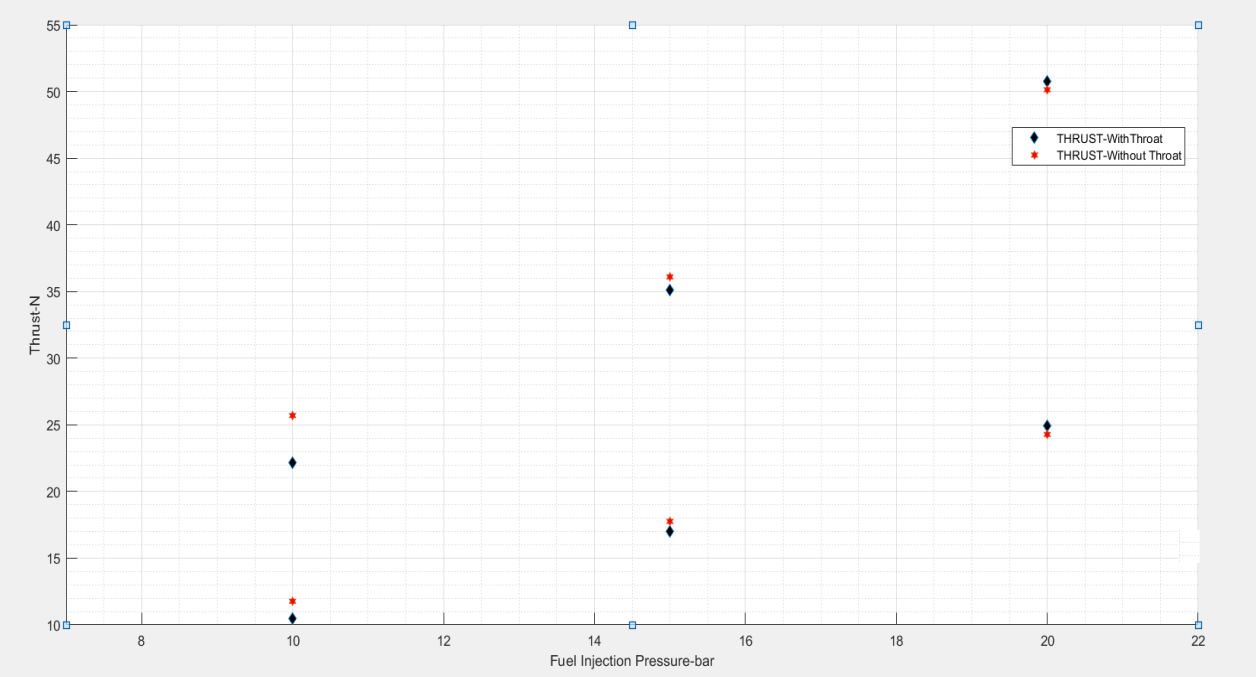

Figure 5:12 A Comparison between Computed values of thrust for test with and without throat section

6 CHAPTER 6

6.1 CONCLUSIONS

A small scaled Rocket Based Combined Cycle Engine was studied in detail with prime focus on the Pure Rocket mode operation. Tests were performed in the facility for varying injection pressure of the reactants, with and without combustion in the Rocket combustion chamber. Data set obtained from the Pressure and temperature sensors was utilized to perform some calculation based on quasi-steady approach. Similar experiments were carried out by changing the geometry of the parametric engine by removing the throat section and the results were compared with the previous ones. The major findings of the study could be summarized as follow:

- A significant Thrust increment due to combustion in the Ramjet combustion chamber is observed as compared to the non-reaction tests.
- Higher injection pressure of the reactants in to the rocket combustion chamber resulted in higher thrust.
- The quasi-steady approach is valid until the supply of both the reactants is present, once the supply of any of the reactants is cut off, system show transient behavior.
- The highest pressure in the Engine (referring to tests with throat) occurs at the Throat section.
- Considering the three different averaging schemes in order to get the average Mach number at the exhaust section of the ramjet, IMAP=0 scheme was found to be the best of all three schemes. It was very interesting to observe that the plain average (the simplest of all) of all the Mach numbers at exhaust also give quite good results comparable with those obtained from IMAP=0.
- The result from the tests performed without throat yielded supersonic flow in the ramjet.
- No significant change in the thrust of the engine was observed during the tests performed with & without throat.

[1] G. Riva, A. Reggiori, and G. Daminelli, “Performance Evaluation of a Ramjet Model in a Pulse Facility at Mach 4.5 | Journal of Propulsion and Power,” *AIAA*, vol. 28, Number 3, pp. 466–476.

[2] R.C. Rogers, D.P. Capriotti, and R.W. Guy, “Experimental Supersonic Combustion at NASA Langley,” presented at the 26th Advanced Measurement and Ground Testing Technilogy Conference, Albuquerque NM, 1998, vol. 1998–2506.

[3] A. Kantrowitz and C. Donaldson, “Preliminary Investigation of Supersonic Diffusers,” presented at the NASA ACR L5D20, 1945.

[4] G. Riva, A. Reggiori, and G. Daminelli, “A NEW PULSE FACILITY FOR STUDIES ON ROCKET-BASED COMBINED CYCLES.,” *Space Technol*, vol. 25, Number 2, pp. 83–92, 2005.

[5] Houghton E. L. and Brock A.E., *Tables for the Compressible Flow of Dry Air*, 3rd ed. London: Edward Arnold Ltd., 1975.